Research Report

Research Project T2695, Task No. 8
Behavior and Design of Joints in Bridge Substructures

SEISMIC BEHAVIOR AND RETROFIT OF BRIDGE KNEE JOINT SYSTEMS

by

David I. McLean
Professor

Nasim K. Shattarat
Graduate Student

Washington State Transportation Center (TRAC)
Washington State University
Department of Civil & Environmental Engineering
Pullman, WA 99164-2910

Washington State Department of Transportation
Technical Monitors
Hongzhi Zhang and Chyuan-Shen Lee
Bridge Engineers

Prepared for

Washington State Transportation Commission
Department of Transportation
and in cooperation with
U.S. Department of Transportation
Federal Highway Administration

July 2005

TECHNICAL REPORT STANDARD TITLE PAGE

1. REPORT NO.	2. GOVERNMENT ACCESSION NO.	3. RECIPIENT'S CATALOG NO.
WA-RD 601.1		

4. TITLE AND SUBTITLE	5. REPORT DATE
SEISMIC BEHAVIOR AND RETROFIT OF BRIDGE KNEE JOINT SYSTEMS	July 2005
	6. PERFORMING ORGANIZATION CODE
7. AUTHOR(S) David I. McLean and Nasim K. Shattarat	8. PERFORMING ORGANIZATION REPORT NO.
9. PERFORMING ORGANIZATION NAME AND ADDRESS Washington State Transportation Center (TRAC) Washington State University Department of Civil and Environmental Engineering Pullman, WA 99164-2910	10. WORK UNIT NO. 11. CONTRACT OR GRANT NO. T2696, Task 8
12. SPONSORING AGENCY NAME AND ADDRESS Washington State Department of Transportation Transportation Building, MS: 7370 Olympia, WA 98504-7370	13. TYPE OF REPORT AND PERIOD COVERED Research Report 14. SPONSORING AGENCY CODE

15. SUPPLEMENTARY NOTES

This study was conducted in cooperation with the U.S. Department of Transportation, Federal Highway Administration.

16. ABSTRACT

Experimental tests were conducted on seven 1/3-scale specimens to define the vulnerabilities of existing outrigger bents under in-plane and out-of-plane seismic loading and to develop appropriate retrofit measures that address the identified vulnerabilities. The specimens represented bents with short and long outrigger beams in the SR-99 Spokane Street Overcrossing in western Washington State. The as-built specimens failed at low ductility levels due to shear distress, low torsional strength of the beam, and reinforcement bond failures within the joint. Circular and D-shaped steel jackets were used to retrofit the regular and split as-built specimens, respectively. The retrofitted specimens developed plastic hinging in the column, with enhanced strength, energy and ductility capacities. Threshold principal tension stress values describing the expected condition of the joints were established and compared to values obtained by other researchers. Design and detailing guidelines for retrofitting outrigger bents were proposed. The guidelines include equations for the jacket thickness required to form a stable force transfer mechanism between the beam and the column reinforcement as well as to prevent joint failure.

17. KEY WORDS	18. DISTRIBUTION STATEMENT
Outrigger bents, Knee joints, Retrofitting, Seismic response, Bond, Shear, Torsion	No restrictions. This document is available to the public through the National Technical Information Service, Springfield, VA 22616.

19. SECURITY CLASSIF. (of this report)	20. SECURITY CLASSIF. (of this page)	21. NO. OF PAGES	22. PRICE
Unclassified	Unclassified	82	

DISCLAIMER

The contents of this report reflect the views of the authors, who are responsible for the facts and accuracy of the data presented herein. The contents do not necessarily reflect the official views or policies of the Washington State Transportation Commission, Washington State Department of Transportation, or the Federal Highway Administration. This report does not constitute a standard, specification, or regulation.

TABLE OF CONTENTS

Page

LIST OF TABLES

LIST OF FIGURES

EXECUTIVE SUMMARY

A number of bridges in Washington State are supported on columns that are offset from the superstructure because of geometric or right-of-way constraints, creating what is referred to as an outrigger bent. Under seismic loading, outrigger bents are subject to gravity forces combined with both in-plane and out-of-plane lateral loads, resulting in complex bending, shear and torsion within the bents. The 1989 Loma Prieta, California earthquake and the 2001 Nisqually, Washington earthquake demonstrated the seismic vulnerability of outrigger knee joint systems, particularly in older, poorly detailed joints, but even in relatively recent construction. As a consequence, there is concern about the performance of knee joints in existing bridges, putting these bridges at risk of partial or even total collapse in a seismic event.

In this study, seven knee joint specimens were tested under simulated seismic loading. These specimens were one-third scale models of selected outrigger bents in the Spokane Street Overcrossing and represented the entire length of the prototype outrigger beam, the knee joint, half the length of the column, and an anchor block simulating the monolithic connection of the beam to the superstructure. The primary objectives of the study were to define the vulnerabilities of outrigger bents under seismic in-plane and out-of-plane loading and to develop appropriate retrofit measures for outrigger knee joints that address the identified deficiencies.

The experimental test results of this study indicate that outrigger bents with reinforcement details typical of those present in the Spokane Street Overcrossing will likely perform poorly in a significant earthquake event. Tests carried out on as-built specimens under in-plane loading showed that shear cracks will form in the joint region

at low displacement levels. Failure will happen as a result of bond splitting of the column reinforcement hook extensions within the joint. The existing outrigger knee joint systems can be expected to achieve ductility levels in the range of 2.0 to 2.8. In the case of out-of-plane motion, the outrigger beams will experience cracking at low displacement levels. Bond splitting failure of the beam reinforcement in the joint with the low torsional strength of the beam will result in the potential for failure of the system.

The retrofit measures developed in this study consisted of an elbow-shaped steel jacket around the beam and the joint region. The retrofitted specimens formed a plastic hinge in a gap introduced at the top of the column with improved ductility, torsional strength, and energy dissipation capacities when compared to the behavior of the similar as-built specimens. The retrofitted outrigger knee joint systems can be expected to achieve ductility levels of at least 5 as well as drift capacities exceeding 6%.

The observed behavior of the knee joints in the as-built specimens was evaluated with respect to the joint principal tension stress levels. Principal tension stress values of $4.5\sqrt{f_c'}$ psi ($0.38\sqrt{f_c'}$ MPa) and $6.0\sqrt{f_c'}$ psi ($0.50\sqrt{f_c'}$ MPa) were set as limits beyond which joint shear cracking and joint failure, respectively, are expected.

Design guidelines for retrofitting outrigger knee bents were proposed, including for knee joints in split bents. The guidelines include recommendations on the jacket thickness required to form a stable force transfer mechanism between the beam and the column and to prevent any potential failure mechanisms in the knee joint and connections members.

INTRODUCTION

INTRODUCTION AND BACKGROUND

A number of bridges in Washington State are supported on columns that are offset from the superstructure because of geometric or right-of-way constraints, creating what is referred to as an outrigger bent. Under seismic loading, outrigger bents are subject to gravity forces combined with both in-plane and out-of-plane lateral loads, resulting in complex bending, shear and torsion within the bents. A complicating factor present in a number of bridges with outriggers in Washington State, including in the Spokane Street Overcrossing, is the presence of splits in some of the bents. Expansion joints are located at the ends of every fourth bent, with a split column being common to both bents in order to accommodate longitudinal movement within the bridge. Typically, a 2-in. (5-cm) gap is incorporated into the split columns. In the outrigger bents, this split carries through the outrigger beams and knee joints, making the development and installation of effective retrofit measures challenging.

The 1989 Loma Prieta, California earthquake and the 2001 Nisqually, Washington earthquake demonstrated the seismic vulnerability of outrigger knee joint systems, particularly in older, poorly detailed joints, but even in relatively recent construction. As a consequence, there is concern about the performance of knee joints in existing bridges, putting these bridges at risk of partial or even total collapse in a seismic event. The purpose of this study was to experimentally investigate the behavior of existing outrigger knee joints under in-plane and out-of-plane loading and to develop retrofit methods for improving the seismic performance of outrigger knee joint systems, including those in split outrigger bents.

RESEARCH OBJECTIVES

The overall goals of this research are to obtain an improved understanding of the seismic behavior of existing knee joints and to develop and evaluate the effectiveness of the retrofit measures for improving their performance in outrigger bents. To achieve these two goals, five objectives were established:

1) Evaluate and define the vulnerabilities of outrigger bents under seismic and gravity loadings;
2) Develop appropriate retrofit measures for outrigger knee joints that address the identified vulnerabilities;
3) Evaluate through experimental testing the feasibility of and benefits resulting from retrofit measures applied to outrigger knee joints;
4) Develop recommendations for the seismic assessment of the existing outrigger knee joints; and
5) Provide design and detailing guidelines for a practical retrofit method for improving the performance and safety of outrigger bents in bridges.

REVIEW OF PREVIOUS RESEARCH

Two significant research studies were conducted in California as a result of the damage that occurred to outrigger bents during the 1989 Loma Prieta earthquake. As-built specimens modeling the actual damaged bridges were tested, and retrofit strategies were then developed and evaluated through further testing.

Ingham et al (1994a, 1994b) investigated the behavior of as-built and retrofitted knee joints under in-plane loading using one-third-scale test specimens. Two as-built

specimens, one representing a bent that performed poorly during the 1989 Loma Prieta earthquake and the second one modeling an outrigger bent with joint reinforcement detailing typical of the 1991 practice in California, were tested. The two as-built specimens performed poorly with low strength, limited energy dissipation capacity and low displacement ductility. Ultimate failure in the first specimen was due to bond failure of the unconfined lap-splice between the vertical hook extensions of the top outrigger beam reinforcement and the longitudinal column reinforcement. The second as-built specimen failed due to inadequate embedment length of the column reinforcement.

Following the tests of the as-built specimens, two retrofit strategies were developed (Ingham et al 1994a, 1994b). The retrofit solution for the first as-built unit utilized external prestressing of the cap beam and joint. This retrofit strategy resulted in improved joint shear strength, but the system ultimately failed in a brittle mode due to high compressive stresses in the joint. The retrofit measure for the second as-built specimen incorporated the use of a lightly reinforced concrete jacket encasing the joint. Testing showed that the retrofitted specimen had more displacement ductility capacity and improved hysteretic behavior than the second as-built specimen.

Stojadinovic and Thewalt (1995) investigated the seismic response of knee joints under combined in-plane and out-of-plane loading and developed upgrade and repair techniques for existing outrigger bents. Two as-built half-scale models, one with a long and one with a short outrigger beam, were constructed and tested. Tests of the as-built specimens showed that both as-built specimens performed in a brittle manner with low force and displacement capacities. Failure in the as-built specimens was due to bond splitting failure in the joint region along with torsion failure in the outrigger beams. Two

upgrade strategies were investigated: a post-tensioned concrete jacket around the beam and the joint, and the addition of flat steel plates connected by through-bolts to the beam and a curved steel plate on the exterior face of the joint. Both retrofits increased ductility and energy dissipation of the outrigger bents. The steel plate solution was easier to construct than the post-tensioned reinforced concrete upgrade.

EXPERIMENTAL TESTING PROGRAM

SPECIMEN DETAILS

The behavior of the knee joint systems in the SR 99 Spokane Street Overcrossing was selected as the focus of this study. The bridge was designed in 1957 probably based on the 1953 AASHO Standard Specifications for Highway Bridges, which did not include any provisions for seismic design or detailing (Zhang et al 1996). Part of the structure consists of cast-in-place reinforced concrete box girders supported on forty-three bents, twelve of which have outrigger knee joints. After reviewing several possible candidates, Bent #20 and bent #36 were selected to characterize regular bents with short and long outrigger beams, respectively. Bent # 34 was selected to represent a split outrigger bent with a long outrigger beam. Figure 1 shows an outrigger bent from the SR 99 Spokane Street Overcrossing.

Figure 1 An Outrigger Bent in the SR 99 Spokane Street Overcrossing.

This study investigated the performance and failure mechanisms of as-built specimens, and retrofits of the outrigger knee joint systems were developed and evaluated. Tests were conducted on 1/3-scale specimens that modeled the entire length of the prototype outrigger beam, the knee joint, half the length of the column, reinforcing ratios and detailing, and material properties. The length of the column in the test setup modeled the length of the prototype column up to the inflection point in the bending moment diagram for the columns under lateral loading. Limits on the weight and ability to handle the specimen made it necessary to substitute part of the concrete column with a steel section of equal stiffness. A stiff anchor block modeled the monolithic connection of the beam to the bridge deck.

A summary of the test specimens is given in Table 1. A total of seven specimens were tested. Details of Specimens ALI and ASI, representing as-built long and short

regular outrigger specimens, are shown in Figures 2 and 3, respectively. Details of Specimen RSPLI are shown in Figure 4. The Washington State Department of Transportation (WSDOT) has already applied steel jackets to the columns in the Spokane Street Overcrossing as a first phase of retrofitting on the bridge. Therefore, the columns in the specimens were retrofitted to replicate the current state of the bridge. The retrofit measures applied to the beam and the knee joint of the remaining specimens are discussed later along with the test results.

Additional details on the test specimens are given by Shattarat (2004).

Table 1 Summary of Test Specimens

Specimen	Description	Load Pattern	Column Upgrade Type	Beam and Joint Upgrade Type
ALI	As-built long outrigger	In-plane	Steel casing	None
ASI	As-built short outrigger	In-plane	Steel casing	None
ASO	As-built short outrigger	Out-of-plane	Steel casing	None
RLI	Retrofitted long outrigger	In-plane	Steel casing	Steel casing
RSI	Retrofitted short outrigger	In-plane	Steel casing	Steel casing
RSPLI	Retrofitted split long outrigger	In-plane	Steel casing	Steel casing
RSO	Retrofitted short outrigger	Out-of-plane	Steel casing	Steel casing

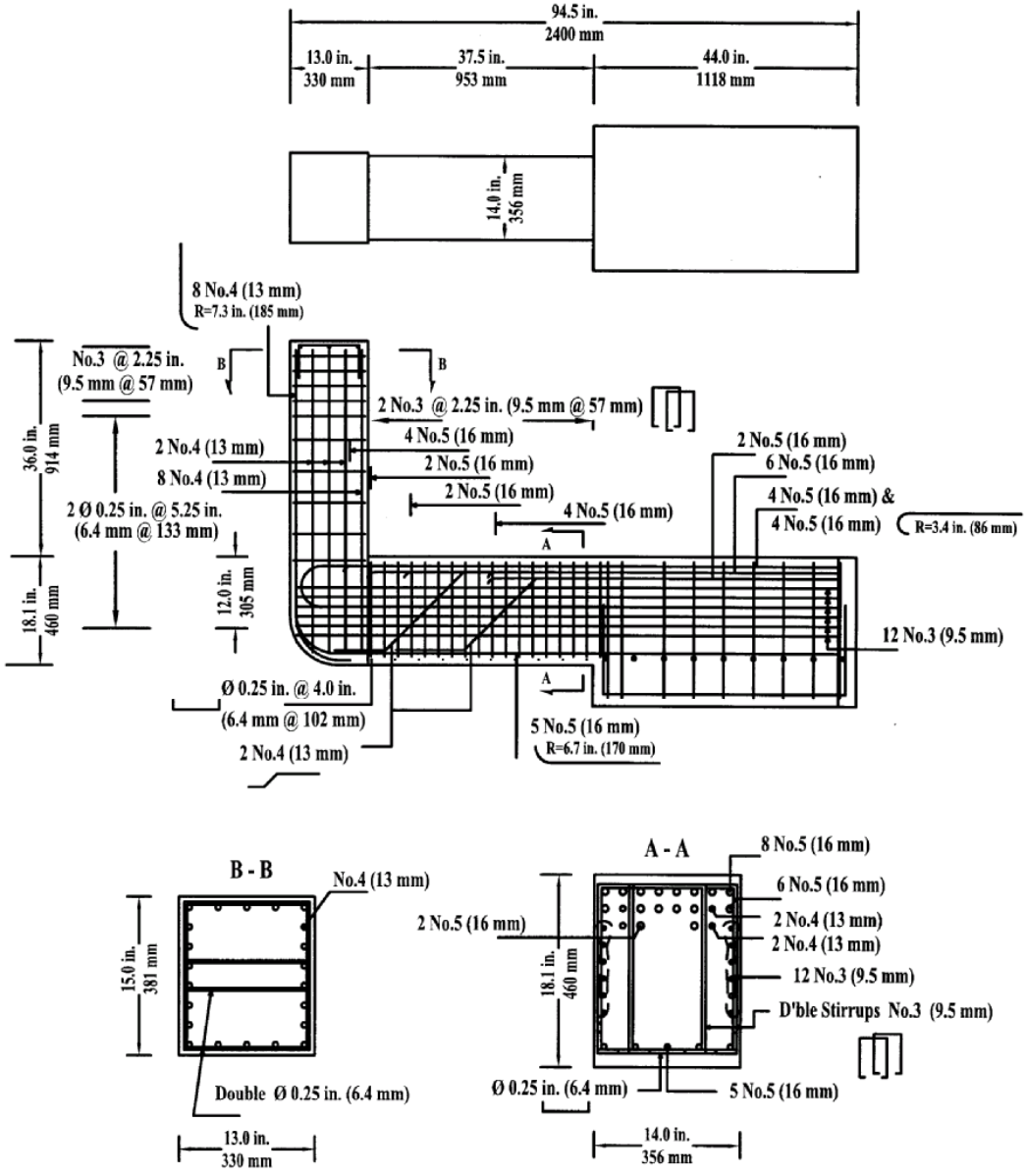

Figure 2 Details of Specimen Representing As-Built Conditions of a Long Outrigger Bent, Specimen ALI.

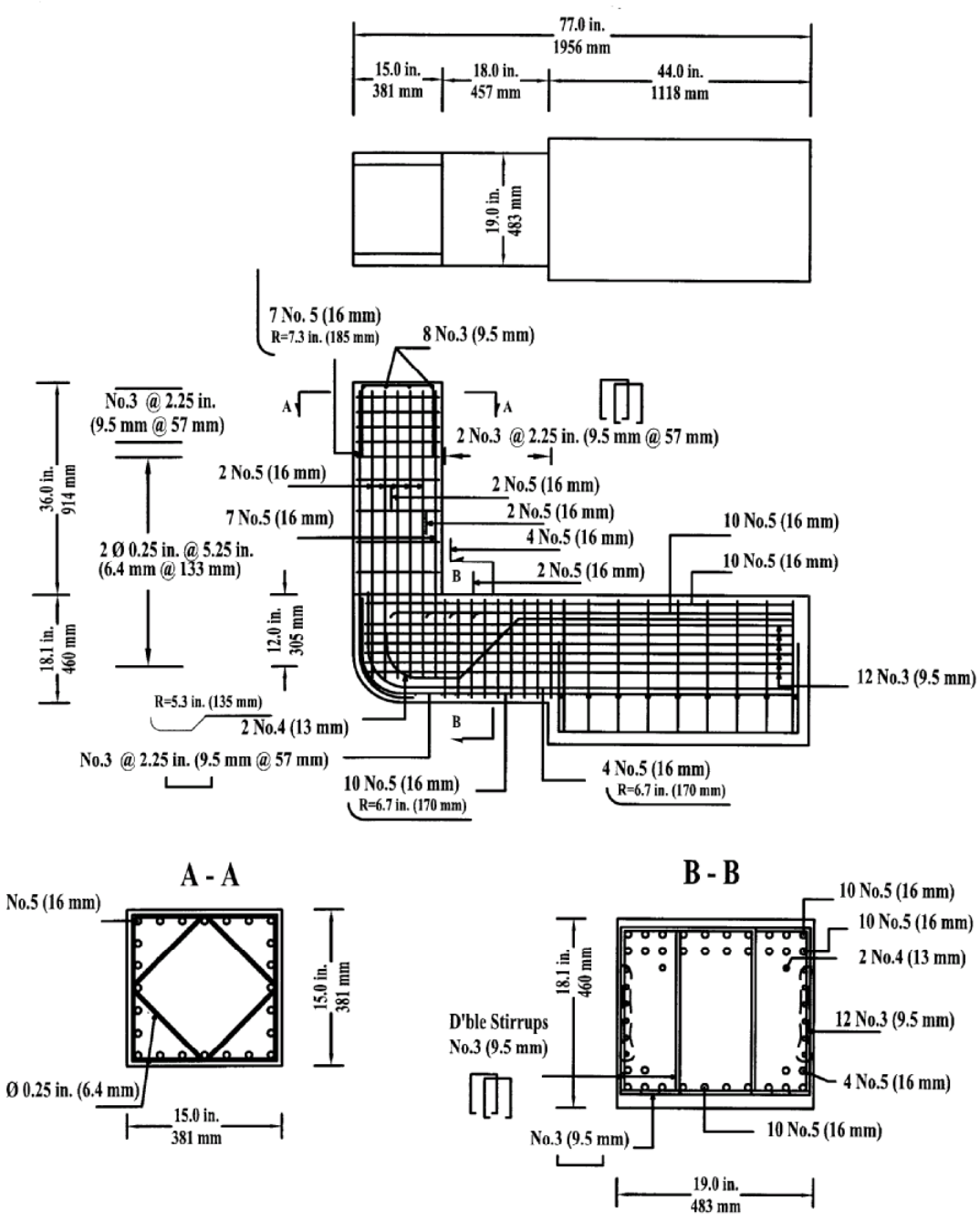

Figure 3 Details of Specimen Representing As-Built Conditions of a Short Outrigger Bent, Specimen ASI.

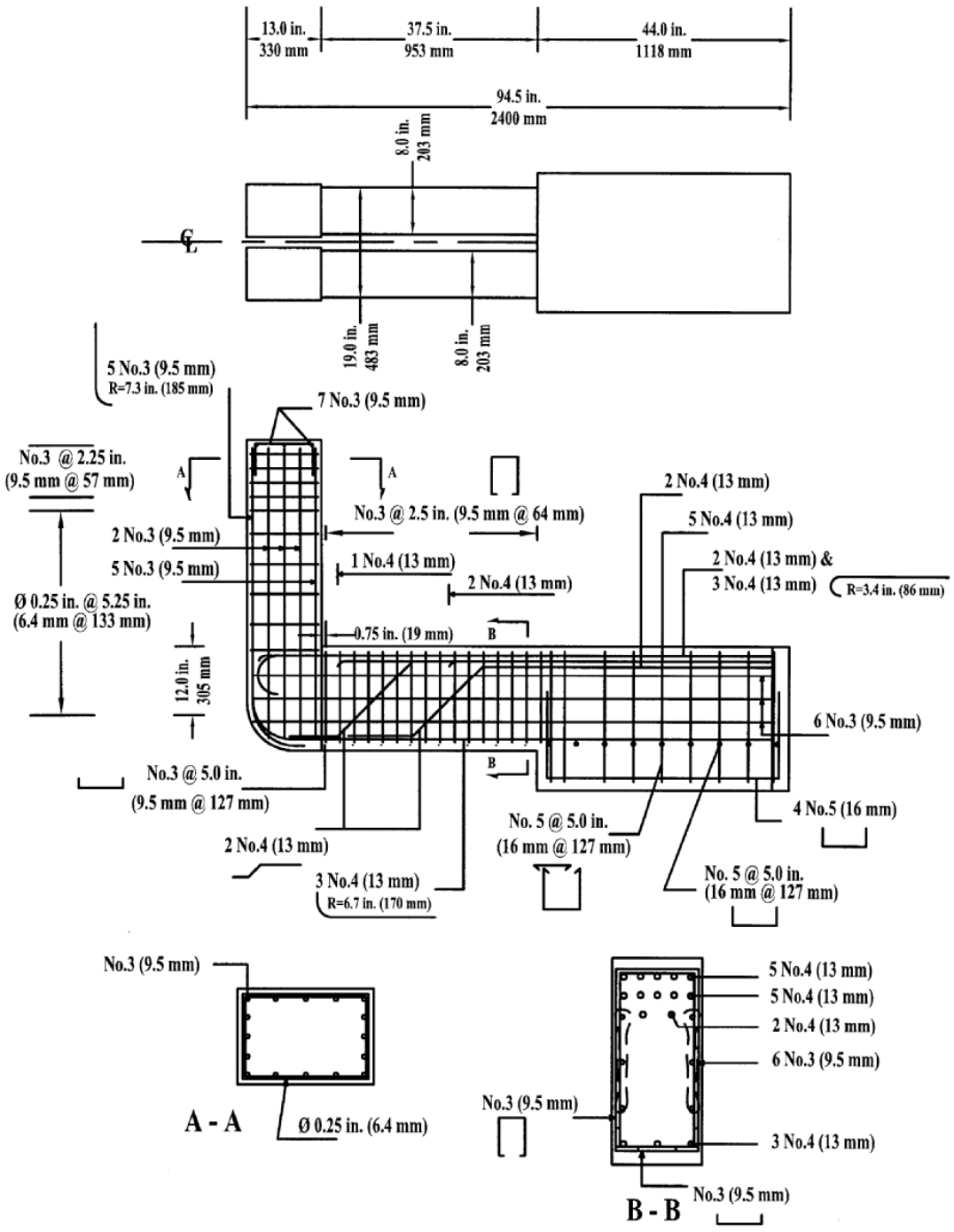

Figure 4 Details of Specimen Representing As-Built Conditions of a Long Split Outrigger Bent, Specimen ASPLI.

TEST SETUP AND PROCEDURES

The in-plane setup of test specimens is shown in Figure 5. The specimens were tested in an upside-down position with respect to the position of the outrigger knee joint in the real structure. The anchor block of the specimen was fixed to the laboratory strong floor. The steel tube section was attached to the top of the concrete column through high-strength embedded anchor bolts. A horizontal 240-kip (1068-kN) capacity actuator reacting against a loading frame was used to apply the horizontal loading pattern. A 200-kip (890-kN) capacity axial load ram provided a constant vertical loading to the top of the column. The axial load ram was attached to a free-sliding trolley with a swivel bolted to the steel plate on top of the tube section. The objective of this test setup was to simulate the in-plane behavior of the outrigger bents under earthquake loading.

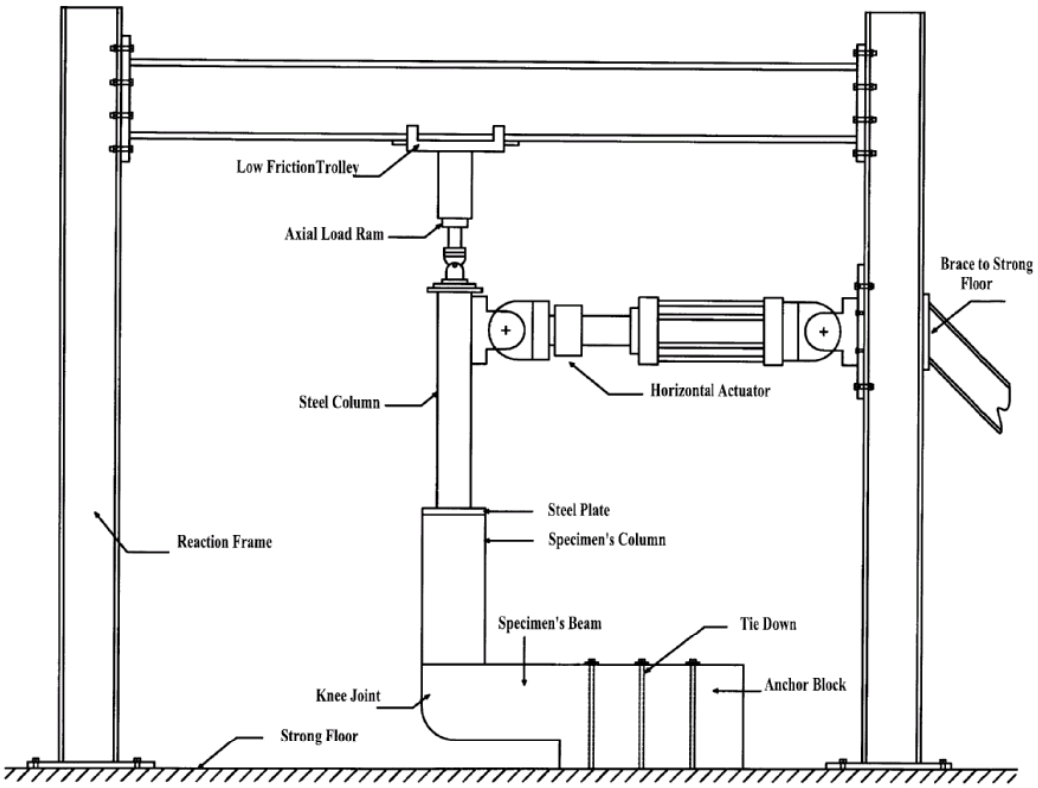

Figure 5 In-Plane Testing Setup.

The out-of-plane setup for the test specimens is shown in Figure 6. In general, the specimen location and anchorage to the strong floor were kept the same as for the in-plane case, except for the actuator, which was rotated 90 degrees to apply a horizontal force perpendicular to the plane of the specimen. This configuration results in out-of-plane bending of the knee joint and simultaneous torsion and weak-axis bending of the beam.

Figure 6 Out-of-Plane Testing Setup.

Axial load levels of 55 kips (245 kN), 33 kips (147 kN) and 27.5 kips (122 kN) were used for short, long and split outrigger specimens, respectively. These load levels correspond to 0.059 $f'_c\ A_g$, 0.041 $f'_c\ A_g$ and 0.028 $f'_c\ A_g$, respectively, where f'_c is the compressive strength of the concrete and A_g is the gross area of the column. The axial load value for each specimen was determined based on the bridge selfweight load carried within the prototype bent and the change in the axial load due to framing action under

opening and closing of the bent. Since the axial load in the testing setup was not varied during testing, a decision was made to model the value of the axial load due to closing moments, resulting in a higher level of demand on the system and thus providing a more conservative estimation of the overall behavior.

Loading of the test specimens was applied in a quasi-static manner. The horizontal loading was displacement controlled based on a pattern of progressively increasing displacements. Curvatures in the beam and the column in the vicinity of the joint interfaces were determined by measuring the difference in extension of two displacement potentiometers mounted on opposite sides of the member. Joint panel instrumentation was mounted on both sides of the joint for the as-built specimens. Five displacement potentiometers on each face were attached to the joint/beam to extract the shear mode of deformation. Stresses in selected reinforcement bars and in the steel jackets of the retrofitted specimens around the joint were measured during testing using strain gages.

TEST RESULTS AND DISCUSSION

The three as-built specimens were tested first: Specimens ALI, ASI, and ASO. These tests revealed the failure mechanisms as well as the force and deformation capacities of the existing outrigger knee joints under in-plane and out-of-plane loading. Results were then used to formulate the retrofit for the subsequent specimens: Specimens RLI, RSI, RSPLI, and RSO.

More detailed discussion of the test results is given by Shattarat (2004).

AS-BUILT SPECIMENS

Specimen ALI

The as-built long outrigger specimen, Specimen ALI, represented a portion of bent #36 in the Spokane Street Overcrossing. Compared to current earthquake-resistant design practice, the confinement and detailing of the joint as well as the beam and the column reinforcement meeting in the joint are unsatisfactory.

A vertical crack associated with opening moments developed at the beam-joint interface while cycling at a displacement level of -1.0 in. (-25 mm). Shear cracks in the joint started to develop while cycling to a displacement level of 1.5 in. (38 mm) combined with vertical cracking on the top corner of the joint resulting from straightening of vertical hook extensions of the bottom beam reinforcement into the joint. Failure in Specimen ALI occurred during cycling to ±3.0 in. (±76 mm) displacement level. The column hook extensions became visible as concrete at the curved side of the joint face spalled off at a displacement level of 2.19 in. (56 mm). At the end of testing, the specimen was still capable of sustaining the applied axial load. Figure 7 shows the damage to the test specimen at the completion of the test.

The resulting actuator force-horizontal displacement history for Specimen ALI is shown in Figure 8. The values of the actuator force corresponding to the theoretical yielding moment, F_Y, and ideal moment, F_I, are shown in the figure. The ideal and yield moment values for the closing direction were calculated based on plastic hinging in the column section at the column-joint interface. In the opening direction, the moment values were based on hinging in the outrigger beam at the beam-joint interface. Figure 6 indicates that the test specimen was able to attain the ideal strength in the closing

direction, but failed to attain even the yield strength in the opening direction. The shape of the force-displacement history shows pinching of the curves near the origin due to cracking of the joint concrete and degradation of the overall performance of the joint. The specimen was able to withstand displacements up to 2.5 in. (64 mm) in both directions before the abrupt drop in the actuator force while looping to close the joint to 3.0 in. (76 mm) displacement level. Specimen ALI was able to attain a maximum ductility level, defined as the maximum attained displacement divided by the yield displacement, of 2.8 at a drift ratio of 3.4% in the closing direction and a maximum ductility of -3.8 at a drift ratio of -3.4% in the opening direction.

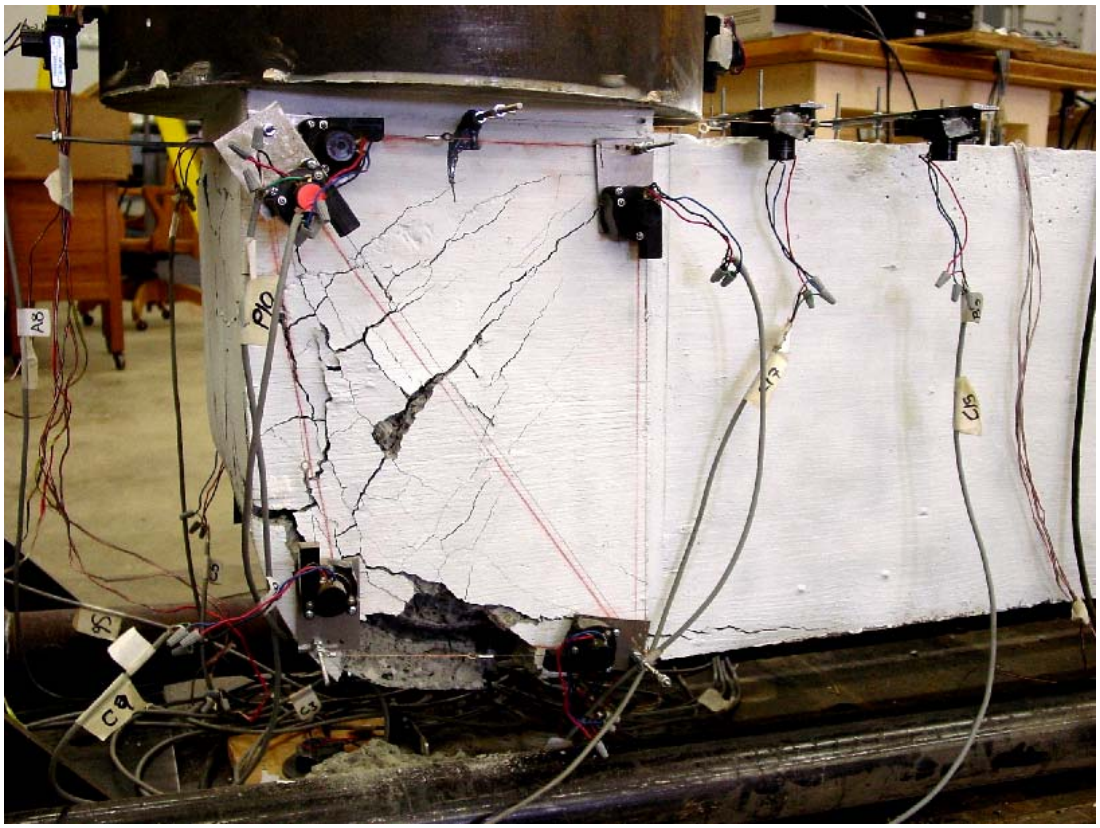

Figure 7 Bond Splitting Failure of the Column Bars in the Joint of Specimen ALI.

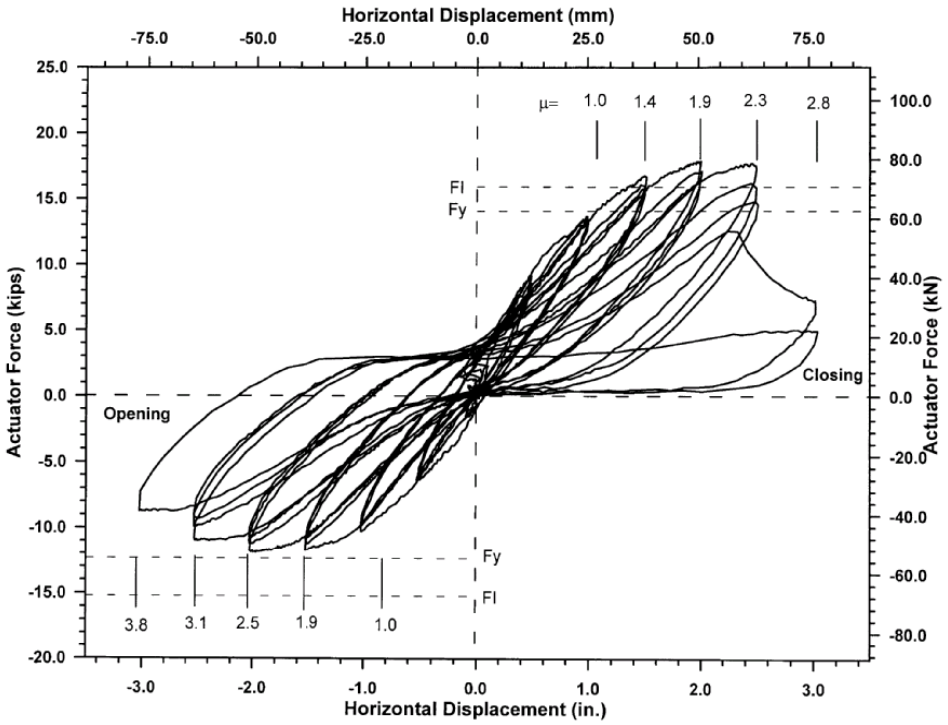

Figure 8 Actuator Force-Horizontal Displacement Curves for Specimen ALI.

The observed behavior of the joint at different stages of the test was linked to the principal tension stress history. The principal tension stress was calculated using a Mohr's circle analysis, as discussed in Priestley et al (1996). It was found that diagonal cracking occurred in the joint region when the principal tension stress exceeded $6.2\sqrt{f_c'}$ psi ($0.52\sqrt{f_c'}$ MPa) in the opening direction and $5.5\sqrt{f_c'}$ psi ($0.46\sqrt{f_c'}$ MPa) in the closing direction. Maximum principal tension stresses of $7.3\sqrt{f_c'}$ psi ($0.61\sqrt{f_c'}$ MPa) and $6.2\sqrt{f_c'}$ psi ($0.52\sqrt{f_c'}$ MPa) were recorded in the joint in the opening and closing directions, respectively, before failure.

Specimen ASI

The as-built short outrigger specimen represented a portion of bent #20 in the Spokane Street Overcrossing.

The earliest noticeable shear cracks on both sides of the joint were observed in the first opening cycle to a displacement level of 1.0 in. (25 mm). Bond failure of the embedded column and beam rebar hook extensions occurred when cycling to the third cycle in the closing direction at a displacement level of 2.7 in. (69 mm). The column and the beam hook extensions exposed as concrete along the free perimeter of the joint from both sides spalled off. The test was stopped following the third closing cycle to a displacement level of 3.0 in. (76 mm) with the specimen still being able to support the applied axial load. Figure 9 shows the damage to the test specimen at the end of the test.

Figure 9 Concrete Spalling as a Result of Splitting Bond Failure of the Column Bars Within the Joint Region of Specimen ASI.

The actuator force-horizontal displacement history for Specimen ASI is shown in Figure 10. The ideal moment, F_I, and theoretical yield moment, F_Y, values were calculated in a similar way as for Specimen ALI. Figure 10 indicates that Specimen ASI reached its yield strength but barely attained the ideal strength in the closing direction. The figure also indicates that in the opening direction the specimen failed to attain the yield strength. The force-displacement hysteresis loops for Specimen ASI show significant pinching due to cracking of the joint concrete. The abrupt drop in capacity caused by the bond splitting failure during joint closing to 3.0 in. (76 mm) displacement level is evident in Figure 10. Specimen ASI was able to attain a maximum ductility level of 2.0 at a drift ratio of 3.4% in the closing direction and a maximum ductility of -3.3 at a drift ratio of -3.4% in the opening direction.

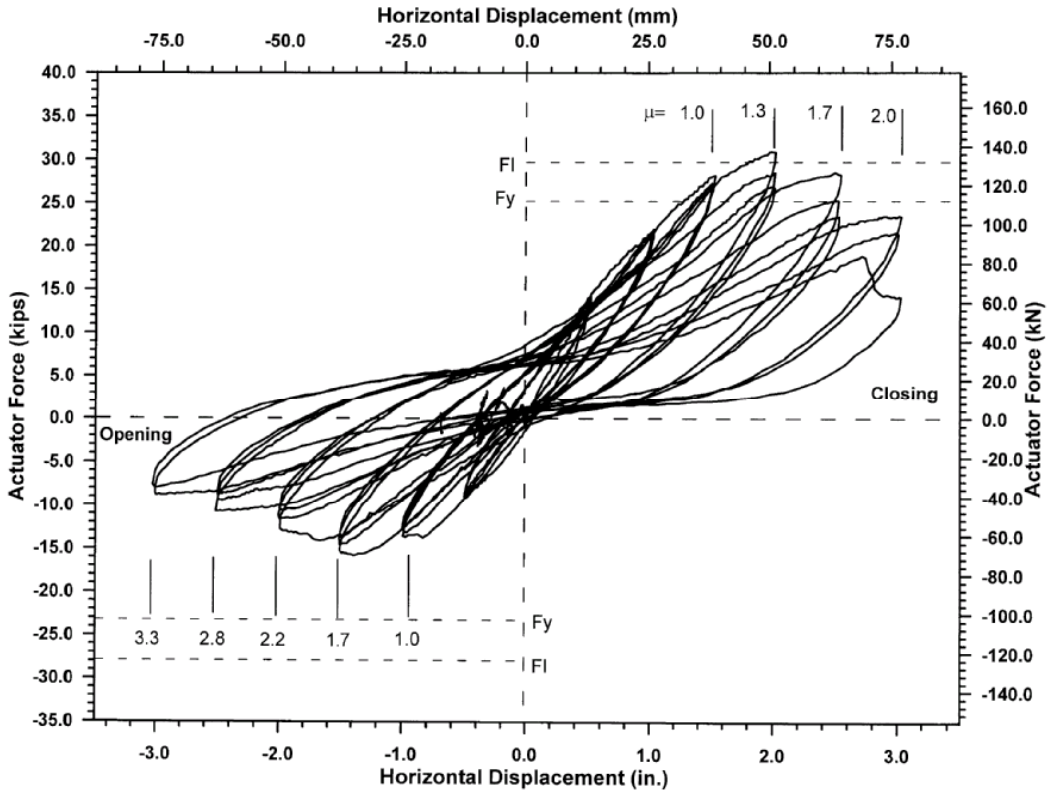

Figure 10 Actuator Force-Horizontal Displacement Curves for Specimen ASI.

Diagonal joint cracking occurred in the opening direction when the principal tension stress exceeded $4.9\sqrt{f'_c}$ psi ($0.41\sqrt{f'_c}$ MPa). The maximum principal tension stress was $7.8\sqrt{f'_c}$ psi ($0.65\sqrt{f'_c}$ MPa) before failure in the opening direction and $8.5\sqrt{f'_c}$ psi ($0.71\sqrt{f'_c}$ MPa) before failure in the closing direction.

Specimen ASO

The detailing of Specimen ASO was identical to Specimen ASI. Specimen ASO was subjected to an out-of-plane loading, while Specimen ASI was tested under in-plane loading. The outrigger beam was reinforced transversely using U-shaped stirrups. Therefore, the torsion capacity of the outrigger beam would be expected to be very close to that of a plain concrete member. The axial load level of Specimen ASO was chosen to be similar to the axial load used in testing Specimen ASI. This load value represented the scenario in which the outrigger bent is taken to a large response under in-plane action with a simultaneous movement in the out-of-plane direction.

The first hairline torsional cracks in the outrigger beam were noticed during the second cycle to 0.5 in. (13 mm) displacement level. Torsional cracks on both faces of the joint with vertical bond split cracks on the back face of the joint developed at a displacement level of ±1.5 in. (±38 mm). The splitting cracks are attributed to the difference in the stiffness between the joint concrete coinciding with the column area and the joint concrete outside that region. During cycling to a displacement level of ±2.5 in. (±64 mm), further opening of the existing torsional and splitting cracks occurred. The test was stopped following the third pull cycle at this displacement level to avoid any damage to the testing apparatus. After the test was completed, the bottom of the

specimen was examined and was found to have large X-shaped torsional cracks, as shown in Figure 11. The large size of these cracks on this face is due to lack of torsional strength and confinement in the section as a result of using U-shaped stirrups.

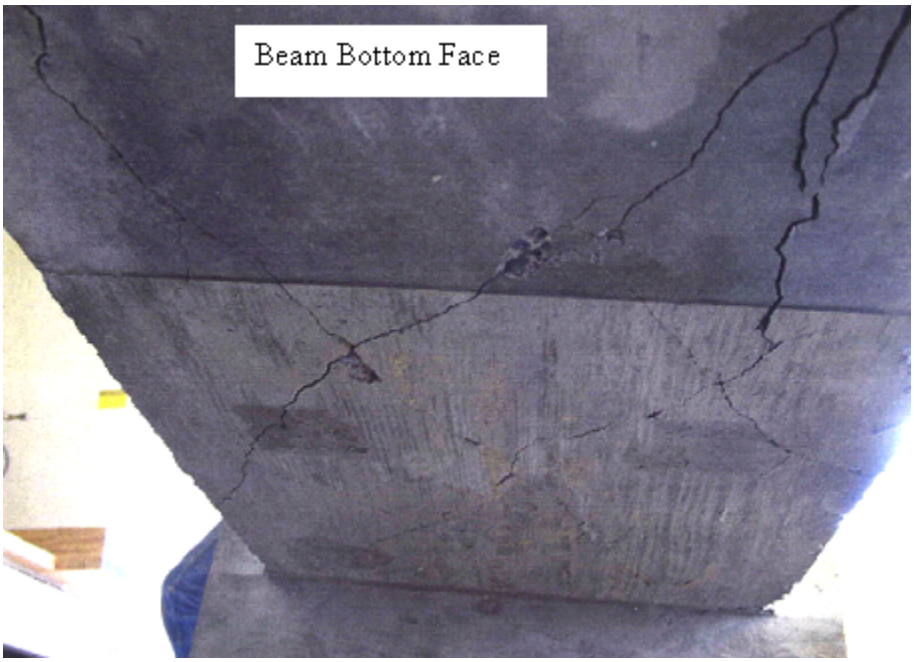

Figure 11 Torsional Cracks in the Beam of Specimen ASO.

The actuator force-horizontal displacement history for Specimen ASO is shown in Figure 12. The value of the actuator force corresponding to the theoretical torsion cracking strength of the outrigger beam, T_{cr}, is shown in the figure. T_{cr} was calculated based on contributions from the concrete and longitudinal steel. Figure 12 indicates that the test specimen was able to attain an average ultimate capacity of 1.68 times the theoretical torsion strength in both directions. Ductilities were not reported for the out-of-plane specimen due to failure mechanism of the specimen, which involved two interacting phenomena: bond splitting and torsion. The hysteresis curves for Specimen ASO, as shown in Figure 12, were relatively narrow, showing little energy dissipation up

to a tip displacement of ±1.0 in. (±25 mm). The specimen exhibited some energy dissipation in the subsequent loops along with some pinching in the last loops to 2.5 in. (64 mm) displacement level due to cracking in the beam and splitting bond failure in the joint region. The specimen was able to withstand displacements of up to 2.0 in. (51 mm) in both directions before a reduction in the actuator force, as shown in Figure 12, corresponding to a drift ratio of 2.5%. A 3.1% maximum drift ratio was reported in both directions at the end of the test.

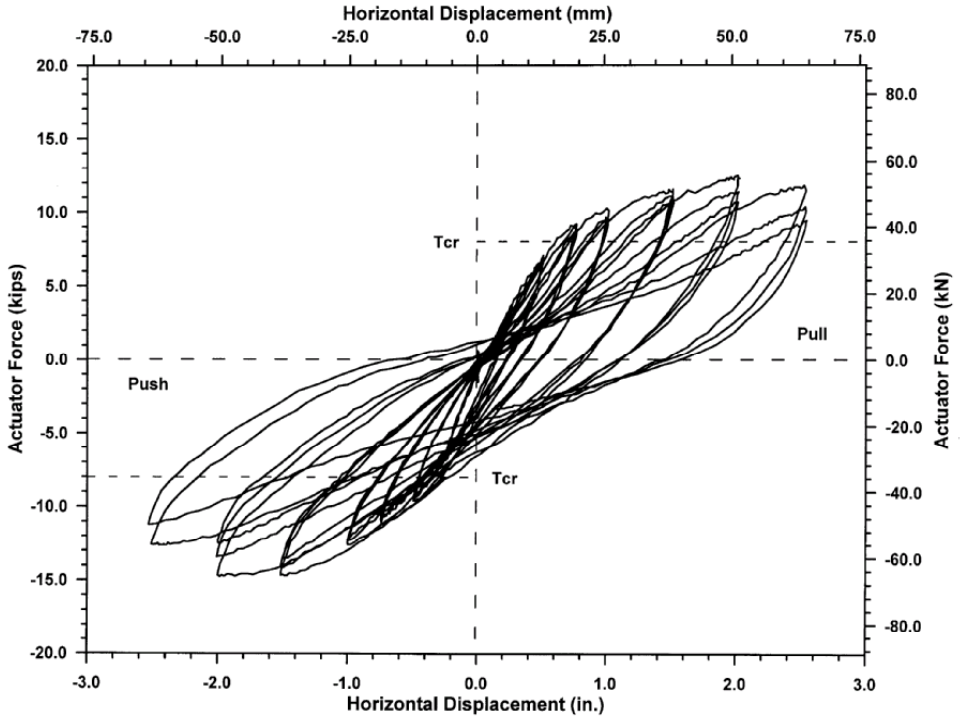

Figure 12 Actuator Force-Horizontal Displacement Curves for Specimen ASO.

Summary of As-built Tests

For in-plane loading, testing showed that the as-built outrigger specimens performed poorly with limited energy dissipation, strength and ductility capacities, due to the damage within the joint. Both the long and the short outrigger specimens were able

to develop the ideal strength of the column in the closing direction, but failed to attain the beam flexural strength in the opening direction. The as-built specimens had a maximum ductility level in the range of 2.0 to 2.8. The two specimens eventually failed in the same manner due to splitting bond failure within the joint region.

In the out-of-plane direction, the as-built specimen experienced diagonal torsion cracking in the outrigger beam and the knee joint during early stages of the test with an ultimate brittle behavior induced by splitting bond failure within the joint region and torsional cracking of the beam. The specimen was able to attain a maximum capacity, on average, 68% higher than the cracking torsion strength in both directions. This substantial increase in the capacity is believed to be due to the behavior of the short outrigger beam transferring forces directly to the anchor block.

RETROFITTED SPECIMENS

Retrofit Description and Design Goals

The main goals of the retrofit measures were to provide for minimal damage in the joint region, improve the torsion capacity of the outrigger beam, enhance the deformation and energy dissipation of the system, be applicable to split outrigger bents, and be feasible to build. These goals were to be achieved by using steel jacketing of the knee joint and the outrigger beam.

The proposed retrofit strategy improves the performance of the outrigger knee joint mainly by providing confinement to the joint region. This confinement is necessary to restrain the column and beam hook extensions in the joint from straightening out and to prevent any potential anchorage failure of the column reinforcement. In addition,

confinement around the joint region provides for the development of a stable force transfer mechanism between the beam and the column reinforcement under opening and closing of the joint.

Circular steel jackets around the beam and the joint were used to upgrade the short and the long outrigger specimens. The steel jacket formed an inverted L-shaped jacket encasing the beam and the joint. The retrofit scheme of the outrigger beam and knee joint was carried out in three steps. First, a ¾-in. (19-mm) gap was provided at a distance of 5.50 in. (140 mm) above the beam-joint interface in the specimen by removing the existing column jacket and the grout in that region. This gap was extended to the depth of the original column. Second, two clamshell sections made of A36 steel with 3/16-in. (4.8-mm) thickness and 24.9-in. (632-mm) diameter were fabricated offsite and welded together in the laboratory using full capacity welding. The clamshell jackets were continuous over the beam and were terminated at a ¾-in. (19-mm) distance from the face of the anchor block.

The clamshells were fabricated by curving a flat plate to form a pipe section with the required length and radius. The pipe was then cut at a 45-degree angle to the required length to jacket the beam. By rotating the leftover piece (eventually forming the joint jacket) in plane by 90-degress, followed by a 180-degree out-of-plane rotation, the piece was then welded to the beam jacket along the 45-degree seam using a full capacity weld forming an elbow shape. The jacket overlapped the existing column jacket above the beam-joint. Finally, the gap between the beam and joint and the steel jacket was filled with high strength grout. Figure 13 shows the dimensions and details of the beam and joint jackets of Specimen RLI.

The split outrigger long specimen was retrofitted in a similar manner but using a D-shaped jacket. First, a ¾- in. (19-mm) gap was provided at a distance of 5.25 in. (133 mm) above the beam-joint interface in the specimen by removing the existing column jacket. This gap was extended to the depth of the original column. Second, Grade A36 rectangular steel plates of 3/16-in. (4.8-mm) thickness were attached to the inner faces of the beam and the joint using high strength epoxy. In the third step, clamshell sections made of A36 steel with 3/16-in. (4.8-mm) thickness were fabricated offsite and welded in the laboratory to the rectangular plates on the inner face of the beam and the joint using a full capacity weld, forming a D-shaped section around the beam and the joint. The clamshell jackets continuous over the beam were terminated at a ¾-in. (19-mm) distance from the face of the anchor block. The joint jacket overlapped the existing column jacket above the beam-joint interface with a lip distance of 1.5 in. (38 mm) over the beam jacket. Finally, the gap between the beam and the joint and the steel jacket was filled by high strength grout. Figure 14 shows the details of the retrofit scheme for Specimen ASPLI.

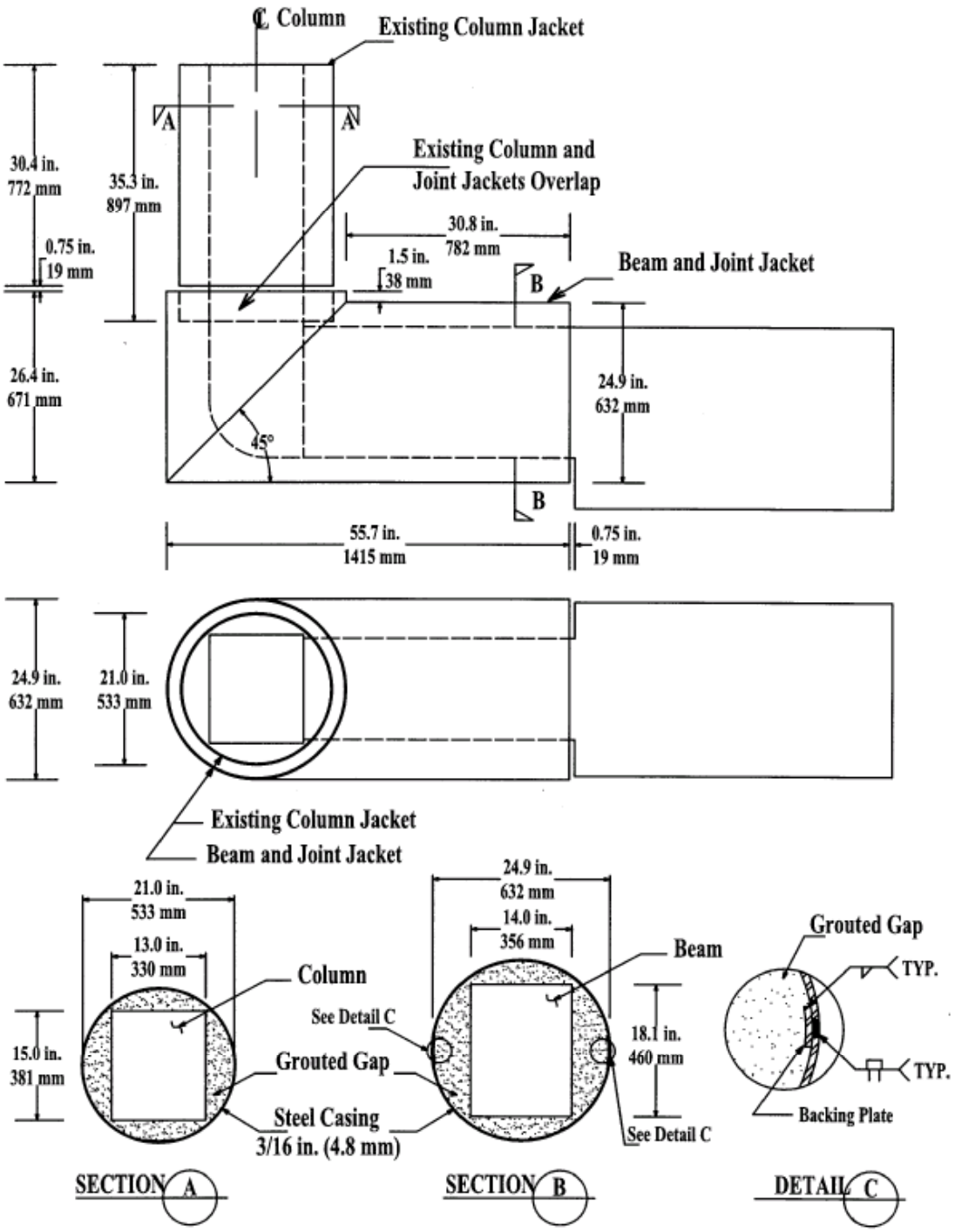

Figure 13 Specimen RLI Retrofit Details.

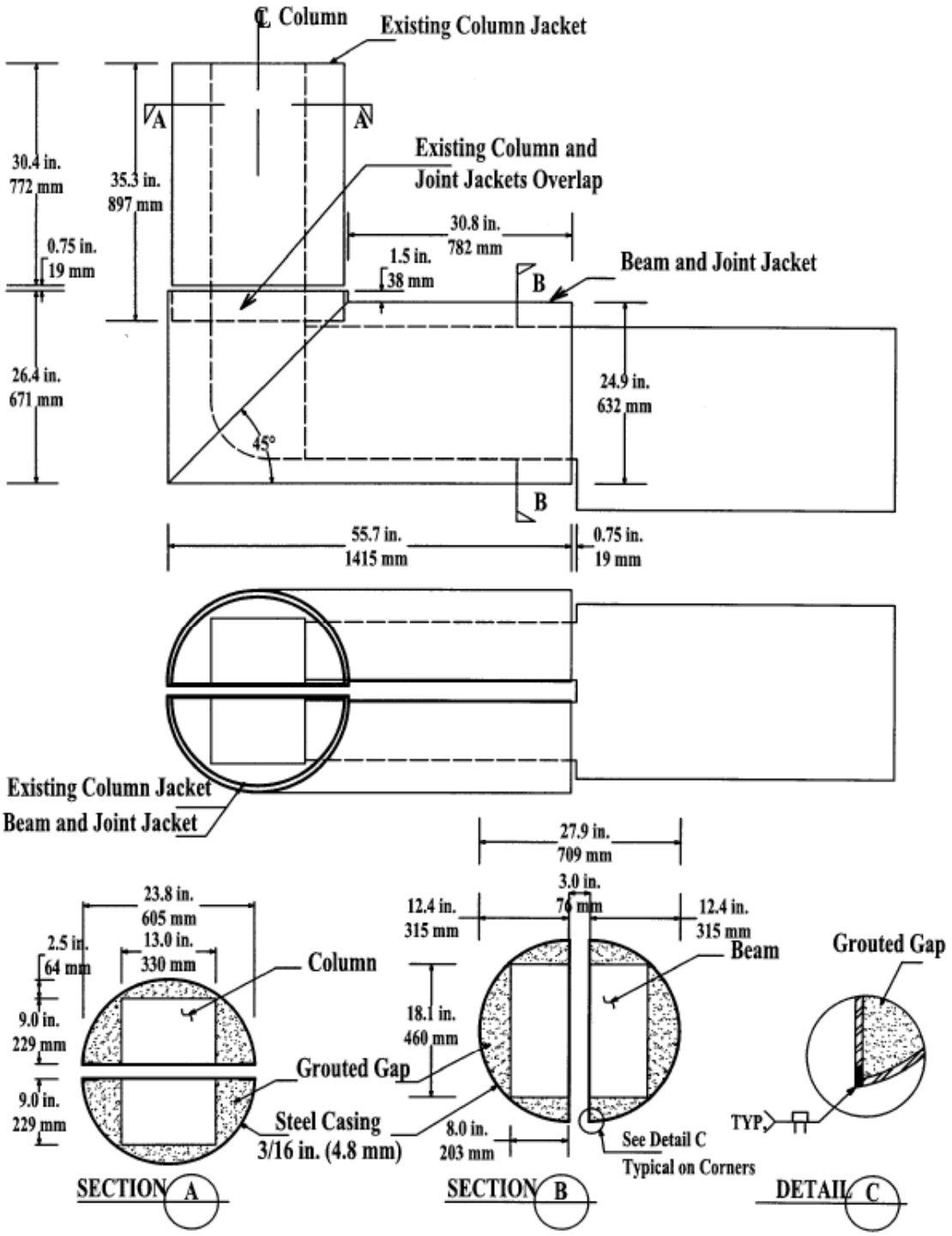

Figure 14 Specimen RSPLI Retrofit Details.

Specimen RLI

Construction and reinforcement details of the as-built portion of the retrofitted long outrigger specimen were nominally identical to Specimen ALI.

The behavior of Specimen RLI was dominated by hinging at the gap location created in the column. The first visible flexure crack in the column gap region attributable to opening moment was noticed during the first cycle to 2.0 in. (51 mm) displacement level. Upon further loading, there was some widening and extension to the existing cracks in the gap area. The column concrete cover within the gap started to spall at a displacement level of 3.5 in. (89 mm) in both directions. The test was stopped following cycles to the 5.0 in. (127 mm) displacement level to avoid any damage to the laboratory loading apparatus. Figure 15 shows a picture of the test specimen at the end of the test. The circumferential strains in the joint jacket of Specimen RLI were well below yielding, with a maximum strain of about 27% of the yield strain.

The hysteresis loops of Specimen RLI are shown in Figure 16. The specimen was able to achieve a 5.0-in. (127-mm) displacement level without any signs of strength degradation. The maximum achieved actuator force was, in average, 48% higher than the ideal strength. This increase in strength occurred due to strain hardening in the column reinforcement and higher concrete compressive strength affected by the confinement provided by the steel jackets. Specimen RLI was able to attain a maximum ductility level of 6.3 at a drift ratio of 6.7% in both directions. These values represent a lower bound estimation of the ductility and drift capacities for Specimen RLI as testing was stopped at the 5.0 in. (127 mm) displacement level before seeing any significant damage to the specimen.

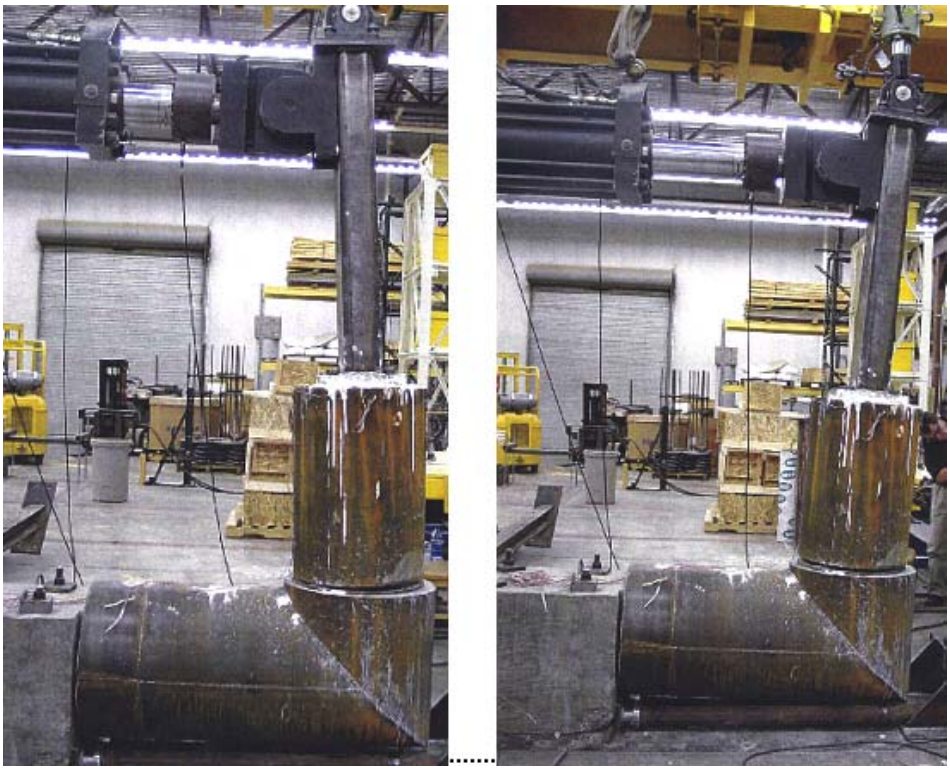

(a) (b)

Figure 15 Specimen RLI at Peak Test Displacements. (a) Closing. (b) Opening.

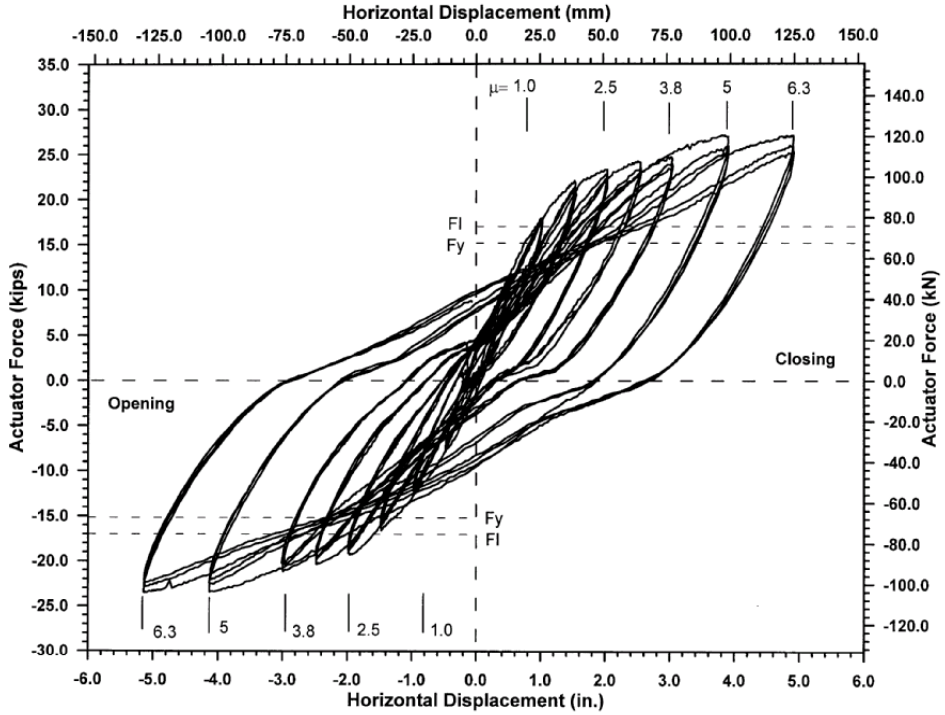

Figure 16 Actuator Force-Horizontal Displacement Curves for Specimen RLI.

Specimen RSI

The as-built portion of Specimen RSI was detailed and constructed as in Specimen ASI. The retrofit measures for the outrigger beam and the knee joint were identical to those used for Specimen RLI. However, the ¾-in. (19-mm) gap was provided at a distance of 5.25 in. (133 mm) above the beam-joint interface and the diameter of the jacket was 27.4 in. (696 mm).

The behavior of Specimen RSI was dominated by hinging at the gap location created in the column. On the cycles to ±2.0 in. (±51 mm) displacement level, there was a flexure crack in the joint gap region during the first cycle to close the joint. Column concrete cover within the gap region started to spall off at a displacement level of 4.0 in. (102 mm) in both directions. The test was stopped following cycles to the 5.0 in. (127 mm) displacement level to avoid any damage to the actuator and the axial load ram. A maximum circumferential strain of about 29% of the yield strain was recorded on the joint jacket.

Figure 17 shows the actuator force-horizontal displacement history for Specimen RSI. The loops were stable up to the end of the test. Specimen RSI was able to achieve a ductility level of 4.6 at a drift ratio of 6.7 % in both directions. Actual ductility and drift capacities will be higher than reported since testing was stopped at 5.0 in. (127 mm) displacement level.

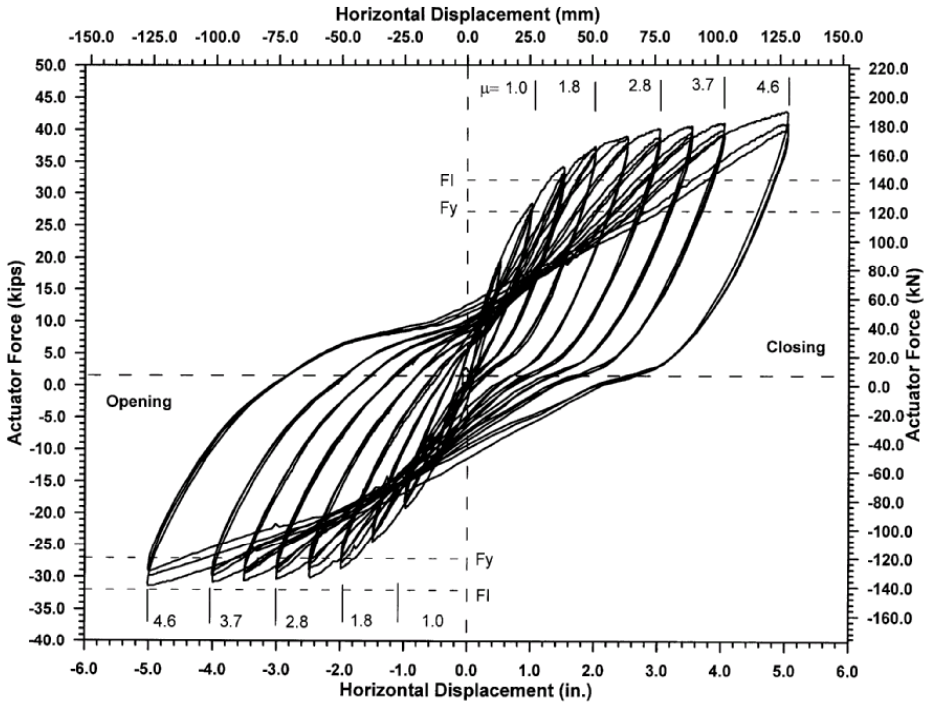

Figure 17 Actuator Force-Horizontal Displacement Curves for Specimen RSI.

Specimen RSPLI

Specimen RSPLI is a retrofitted split long outrigger specimen and is a scaled retrofit of bent #34 in the Spokane Street Overcrossing. Figure 18 shows an overall view of Specimen RSPLI.

The earliest signs of flexural cracking in the column gap region were observed in the first cycle to 1.5 in. (38 mm) in the closing direction. Upon further loading, and during the third cycle to 2.0 in. (51 mm) displacement level, a flexure crack formed in the gap region as a result of joint closing. The concrete cover on the corners of the column started to crush and spall at a displacement level of 4.0 in. (102 mm) in both directions. The test was concluded at the 5.0 in. (127 mm) displacement level to avoid any damage to the laboratory testing apparatus. Some slippage of the added retrofit jacket over the

existing column jacket was observed during testing. This slippage likely happened due to a reduction in confining pressure around the joint region as a result of out-of-plane bending of the flat back plates within the split forming the D sections. Strain gages were positioned on both split knee joints jackets in the Specimen RSPLI with values showing similar behavior. The maximum strain value was measured as 33% of the yield strain.

Figure 18 Overall View of Specimen RSPLI.

The actuator force-horizontal displacement history is shown in Figure 19. It is evident from Figure 19 that the Specimen RSPLI experienced substantial energy dissipation while looping to 4.0 in. (102 mm) and 5.0 in. (127 mm) displacement levels.

Strain hardening and confinement effects pushed the hysteresis loops above the specimen ideal strength. The specimen was able to achieve a 5.0-in. (127-mm) displacement level without any signs of strength degradation. Specimen RSPLI was able to attain a maximum ductility level of 6.4 at a drift ratio of 6.7% in both directions. Similar to the other retrofitted specimens, RLI and RSI, these values represent a lower estimation of the ductility, drift, and strength capacities for Specimen RSPLI, as testing was stopped at a 5.0-in. (127-mm) displacement level.

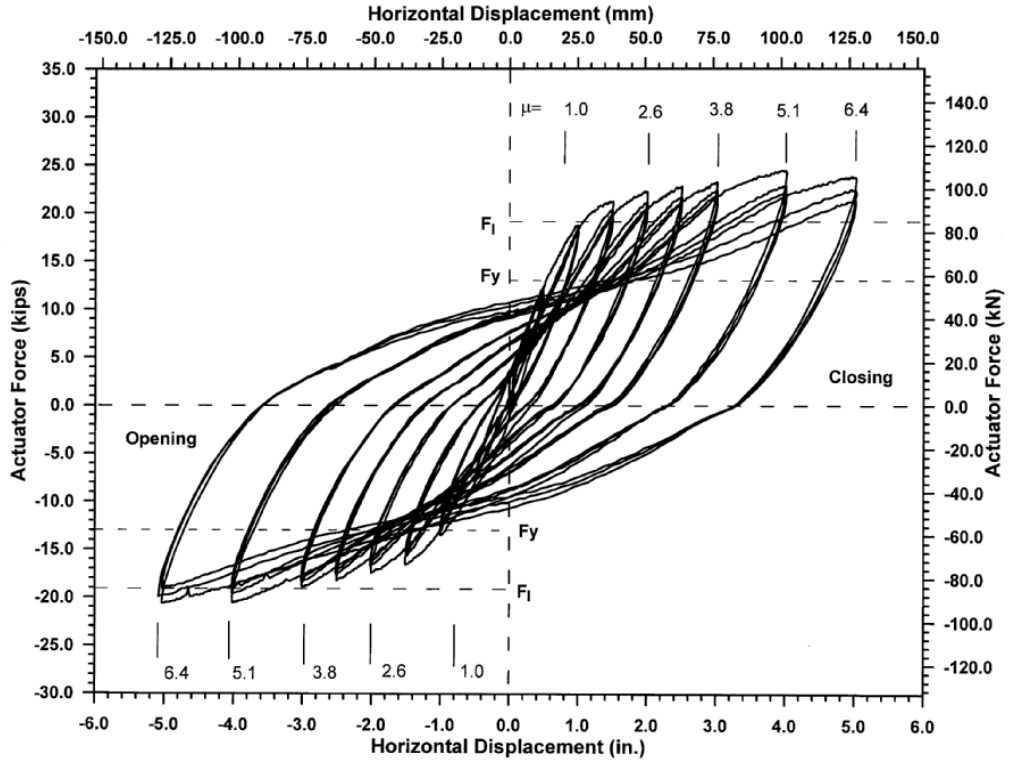

Figure 19 Actuator Force-Horizontal Displacement Curves for Specimen RSPLI.

Specimen RSO

Specimen RSO was a retrofitted model of bent #20 in the Spokane Street Overcrossing. The specimen was retrofitted in the same fashion as Specimen RSI, but

was tested under out-of-plane loading. Figure 20 shows an overall view of Specimen RSO.

Figure 20 Overall View of Specimen RSO.

Testing was stopped following cycles to 76 mm (3.0 in.) displacement level to avoid any damage to the actuator and the axial load ram. This is ½-in. (13-mm) higher than the maximum displacement level in the comparable unretrofitted Specimen ASO. Observations were made of two critical sections of Specimen RSO during the out-of-plane testing: the new ¾-in. (19-mm) column gap, and the region where the outrigger beam connects to the anchor block. Testing showed no cracking in these sections. The column in the specimen behaved as a cantilever with a fixed support at the knee joint. Consequently, the specimen was expected to experience some cracking in the column gap region if testing were taken to higher responses. The maximum circumferential strains in

the joint jacket of Specimen RSO were well below yielding, about 12% of the yield strain.

The actuator force-horizontal displacement history is shown in Figure 21. It is apparent from the figure that the calculated column ideal strength was not reached in either direction due to the test being stopped early, at the 3.0 in. (76 mm) displacement level. The hysteresis loops of Specimen RSO show a small increase between subsequent displacement levels. The specimen was able to achieve a 3.0-in. (76-mm) displacement level at a drift ratio 3.75% without any signs of strength degradation. These values represent a lower estimation of drift and strength capacities as testing was stopped early, without witnessing any damage to the specimen.

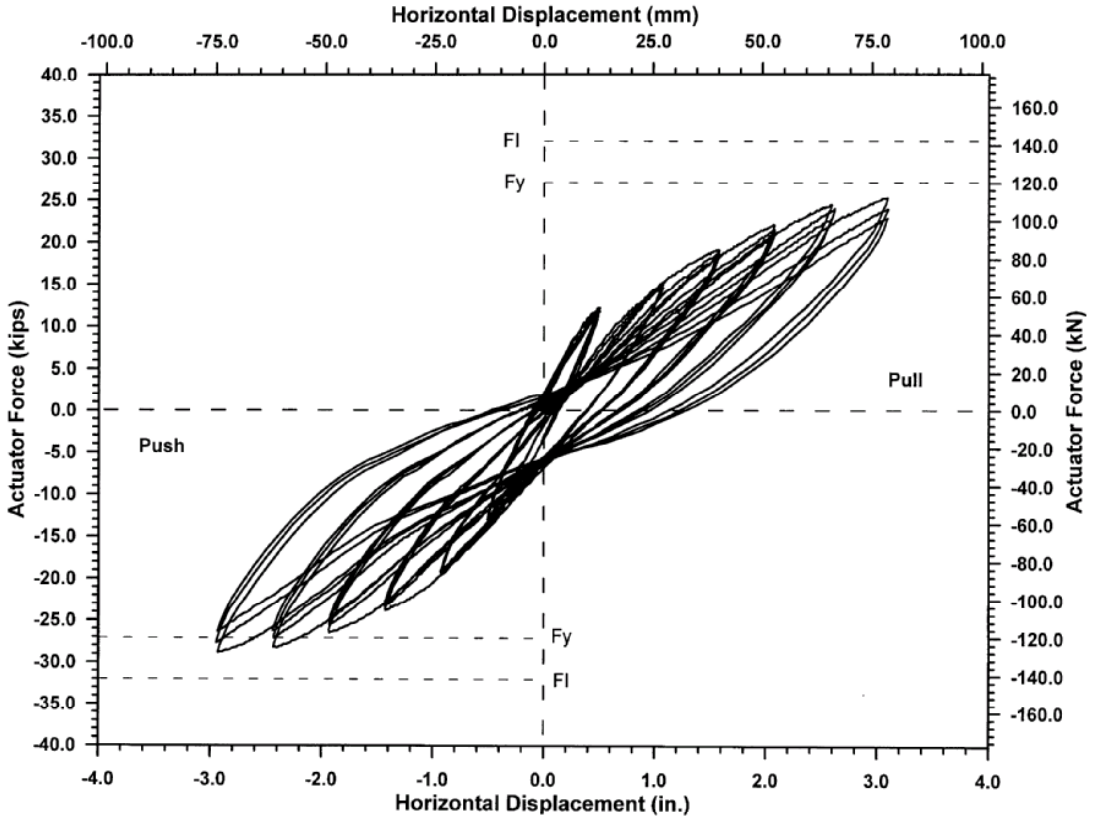

Figure 21 Actuator Force-Horizontal Displacement History for Specimen RSO.

Summary of Retrofitted Tests

Testing of the retrofitted specimens under in-plane loading showed that ductile plastic hinges formed within the columns in the introduced gap region. Ductility levels of 6.3, 4.6, and 6.4 were attained for the retrofitted long outrigger, retrofitted short outrigger, and retrofitted long split outrigger, respectively. These ductility values correspond to the maximum testing displacement level. Higher ductility values would be anticipated if the specimens were tested to greater displacements. For the long and the short specimens, the retrofitted specimens maintained their capacity up to the end of testing with no signs of strength degradation, and they had maximum strengths that were approximately 50% greater than those of the comparable as-built specimens in the closing direction. In the joint opening direction, the retrofitted short and long outrigger specimens developed strengths approximately twice that of the as-built specimens. This larger difference in the opening direction was due to the difference in the member controlling the flexural behavior: the beam in the as-built specimens and the column in the retrofitted specimens.

In the out-of-plane direction, the retrofit measure added significantly to the system capacity and stiffness. In particular, the jacket of the specimen significantly increased the torsion capacity of the beam. The retrofitted specimen reached twice the capacity of the as-built specimen without any sign of strength deterioration, up to the maximum testing displacement level, 3.0 in. (76 mm), with stable force-displacement and energy dissipation behavior in both directions. Greater displacement and strength capacities would have been achieved if the retrofitted specimen had been tested at higher response.

SEISMIC ASSESSMENT OF EXISTING BRIDGE KNEE JOINTS

INTRODUCTION

Design and detailing guidelines for new reinforced T-joints and reinforced knee joints are available in the ACI 318-02 (2002) Building Code and AASHTO Specifications (2004). The 2004 Caltrans Seismic Design Criteria (SDC) provides a basis for design and detailing of reinforced T-joints, but still considers knee joints as nonstandard elements where design criteria need to be developed on a project-specific basis. Strength and deformation of nominally unreinforced knee joints in building frames are discussed in the 1997 National Earthquake Hazard Rehabilitation Program (NEHRP) Guidelines for the Seismic Rehabilitation of Buildings (FEMA-273). For nominally unreinforced bridge knee joints, strength and deformation are discussed by Priestley et al (1996).

Seismic assessment of nominally unreinforced knee joints can be carried out by comparing the demand actions on the joint with the design requirements in Priestley's recommendations. These recommendations consider joint principal tension and compression stresses as criteria for joint design. Maximum joint principal tension and compression stresses can be calculated based upon the assumption of a uniform stress distribution using a Mohr's circle analysis (Priestley et al 1996).

ASSESSMENT OF EXISTING KNEE JOINTS

Traditionally, code provisions and design guidelines adopt a nominal joint shear stress level as a parameter for the design of beam-column joints of building frames and

bridges. Among those are the current ACI 318-02 Building Code (2002), the FEMA-273 document (1997), and the AASHTO Specifications (2004). Other guidelines such as Caltrans SDC (2004) and Priestley's recommendations (Priestley et al, 1996) consider joint principal tension and compression stresses as criteria for joint design. The logic behind using principal stresses rather than nominal shear stresses is that the joint is unlikely to experience shear distress if the average principal tension stress is less than the tensile strength of the joint concrete (Priestley et al, 1996).

The nominal joint shear stress, v_j, can be calculated by dividing the shear force, V_j, determined based on the ultimate flexural capacity of the member controlling the flexural behavior in the opening and the closing direction, by the effective horizontal joint area, A_j. Thus:

$$\upsilon_j = \frac{V_j}{A_j} \qquad \text{(Equation 1)}$$

Based on FEMA-273 (1997), A_j is defined by a depth equal to the column dimension in the direction of framing and a width equal to the smallest of the column width, the joint depth plus the beam width or twice the smaller perpendicular distance from the longitudinal axis of the beam to the column side. Priestley et al (1996) define the effective joint shear area as a depth equal to the column dimension in the direction of framing and a width taken at the center of the column, allowing 45º spread from boundaries of the column section into the cap beam. This definition of A_j is largely based on engineering judgment (Priestley et al, 1996). For comparison, the effective joint area was computed for the as-built long and short outrigger specimens of this study following the definitions in both references. For the as-built long and short specimens, the joint dimensions, depth by width, are 13.0 in. (330 mm) by 15.0 in. (381 mm) and 15.0 in.

(381 mm) by 19.0 in. (483 mm), respectively, calculated as defined in both references. Thus, it can be concluded that the effective joint shear area for knee joints where the beam centerline passes through the column centroid is the same based on both FEMA-273 and Priestley's recommendations.

Based on FEMA-273 (1997), the performance of an existing knee joint can be evaluated by comparing the shear stress demand on to the shear stress capacity of the joint, v_n, as described below.

$$\upsilon_n = \gamma\sqrt{f_c^{'}(psi)} = \frac{\gamma}{12}\sqrt{f_c^{'}(MPa)} \qquad \text{(Equation 2)}$$

where γ is a coefficient for joint shear strength based on the volumetric ratio of horizontal confinement in the joint, ρ'', as shown in the following table.

Table 2 Values of γ for Knee Joint Strength Calculation (Adapted from FEMA-273, 1997).

ρ''	γ
< 0.003	4
≥ 0.003	8

Following Priestley's recommendations, joint principal tension stress is the parameter used to evaluate the performance of an existing knee joint. The joint normal axial and vertical stresses need to be determined in addition to joint shear stress. Using the beam axial force, P_b, the normal horizontal stress, ρ_x, based on Priestley et al (1996), can be determined by:

$$\rho_x = \frac{P_b}{A_b} \qquad \text{(Equation 3)}$$

where A_b is the outrigger beam gross sectional area. Joint vertical axial stress, ρ_y, is determined using the following equation:

$$\rho_y = \frac{P_c}{b_{je}(h_c + 0.5h_b)} \qquad \text{(Equation 4)}$$

where b_{je} is an effective width taken at the center of the column, allowing 45º spread from boundaries of the column section into the cap beam. This is identical to the effective width defined for joint shear area. The joint depth, $(h_c + h_b/2)$, used for vertical stress calculations is based upon dispersion of the column axial force into the outrigger beam at 45° (Priestley et al, 1996). Once the joint shear stress and horizontal and vertical normal stresses are known, the maximum joint principal tension, ρ_t, and compression, ρ_c, stresses can be calculated based upon the assumption of a uniform stress distribution using a Mohr's circle analysis:

$$\rho_c, \rho_t = \left(\frac{\rho_x + \rho_y}{2}\right) \pm \sqrt{\left(\left(\frac{\rho_x + \rho_y}{2}\right)^2 + v_j^2\right)} \qquad \text{(Equation 5)}$$

Using Priestley's recommendations, the performance of the knee joint is then assessed by comparing the principal tension demand on the joint to the principal tension stress ranges given in Table 3.

The stress values presented in the Table 3 are based on work done by Ingham, Priestley and Seible (1994a) on existing knee joint systems with rectangular columns where a maximum joint principal tension stress of approximately $5.8\sqrt{f_c'}$ psi ($0.48\sqrt{f_c'}$ MPa) was achieved before joint failure. This corresponds to a nominal shear stress of about $8.0\sqrt{f_c'}$ psi ($0.66\sqrt{f_c'}$ MPa). Later on, Ingham (1995) proposed a slightly different

limiting joint principal tension stress of $6.0\sqrt{f_c'}$ psi ($0.50\sqrt{f_c'}$ MPa), beyond which joint failure occurs.

Table 3 Existing Knee Joint Assessment Based on Priestley et al (1996)

Principal Tension Stress	Condition
$3.5\sqrt{f_c'(psi)} \le p_t \le 5.0\sqrt{f_c'(psi)}$ $0.29\sqrt{f_c'(MPa)} \le p_t \le 0.42\sqrt{f_c'(MPa)}$	Joint shear cracking
$p_t \ge 5.0\sqrt{f_c'(psi)}$ $p_t \ge 0.42\sqrt{f_c'(MPa)}$	Joint failure

Results from this study on the tests of the as-built specimens under in-plane loading provided the opportunity to review the values proposed by Priestley et al (1996) and update them if appropriate. The values presented by Priestley et al (1996) were based upon a single test on an as-built specimen with nominally unreinforced knee joint under in-plane loading. Table 4 summarizes the joint principal tension stresses and the related joint condition obtained from tests on the as-built long and short outrigger specimens under in-plane loading. Principal tension stresses correspond to the minimum anticipated in the closing and the opening directions.

Based on the stress values obtained from tests presented in Table 4, principal tension stress values of $4.5\sqrt{f_c'}$ psi ($0.38\sqrt{f_c'}$ MPa) and $6.0\sqrt{f_c'}$ psi ($0.50\sqrt{f_c'}$ MPa) are proposed as limits beyond which joint shear cracking and joint failure, respectively, are expected.

Table 4 Joint Principal Tension Stresses for the As-Built Long and Short Specimens

Specimen	Principal Tension Stress	Condition
As-built long	$5.5\sqrt{f_c'}\,psi(0.46\sqrt{f_c'}\,MPa)$	Joint shear cracking
	$6.2\sqrt{f_c'}\,psi(0.52\sqrt{f_c'}\,MPa)$	Joint failure
As-built short	$4.9\sqrt{f_c'}\,psi(0.41\sqrt{f_c'}\,MPa)$	Joint shear cracking
	$7.8\sqrt{f_c'}\,psi(0.65\sqrt{f_c'}\,MPa)$	Joint failure

Table 5 Proposed Principal Tension Stress Values for Knee Joint Assessment

Principal Tension Stress	Condition
$4.5\sqrt{f_c'}\,psi \le p_t \le 6.0\sqrt{f_c'}\,psi$ $0.38\sqrt{f_c'}\,MPa \le p_t \le 0.50\sqrt{f_c'}\,MPa$	Joint shear cracking
$p_t \ge 6.0\sqrt{f_c'}\,psi$ $p_t \ge 0.50\sqrt{f_c'}\,MPa$	Joint failure

The threshold principal tension stresses proposed for knee joint assessment based upon results from this study, shown in Table 5, are slightly higher than those proposed by Priestley, shown in Table 3. The difference in the values is believed to be due to the presence of longitudinal side reinforcement in the joint region as beam skin reinforcement extended into the joint. In the knee joint test conducted by Ingham et al (1994a), which formed the basis for Priestley's recommendations for existing knee joint assessment, the beam side reinforcement was terminated at the beam joint interface. Therefore, it is suggested that knee joints with no side reinforcement be assessed based

upon the threshold principal tension stresses proposed by Priestley, as given in Table 3. For other cases, in which the beam skin reinforcement is fully developed into the joint region and the longitudinal reinforcement ratio is close to those present in the tested specimens in this study (0.45%), the principal tension stresses in Table 5 may be used.

ASSESSMENT OF EXISTING OUTRIGGER BEAMS

Testing of the short outrigger beam specimen under out-of-plane loading highlighted the vulnerability of the outrigger beam when subject to combination of bending, torsion and shear stresses. The initial cracking pattern on the outrigger beam's surfaces in the joint vicinity, which developed at nearly at a 45-degree angle, indicates that formation of these cracks happened primarily due to shear and torsion stresses. In this section, a principal tension stress is suggested as a limit to the onset of cracking in the beam. In addition, an ultimate torsional strength value is proposed as a multiple of the torsional cracking strength for short outrigger beams.

Table 6 shows the principal tension stress at which cracking in the outrigger beam was experimentally observed. The outrigger beam in this study was able to attain an ultimate torsional strength capacity that was 68%, higher, on average, than the cracking torsion strength in both directions, T_{cr}, before the longitudinal resistance of the knee joint system started to diminish. T_{cr} was computed based on the work of Hsu (1990). Consequently, a value of 1.5 T_{cr} is proposed as a conservative estimate of the ultimate torsional strength, T_n, of an existing outrigger beam.

$$T_n = 1.5\left[T_{cr} = 6(x^2 + 10)y\sqrt[3]{f_c'}[1.00 + 4(\rho_L + \rho_h)]\right] \quad (in.; psi) \qquad \text{(Equation 6a)}$$

$$T_n = 1.5\left[T_{cr} = 678(x^2 + 10)y\sqrt[3]{f_c'}[1.00 + 4(\rho_L + \rho_h)]\right] \quad (mm; MPa) \qquad \text{(Equation 6b)}$$

where x = smaller dimension of the rectangular section, y = larger dimension of the rectangular section, $f_c^{'}$ = compressive strength of the concrete, and ρ_L, ρ_h = volume ratio of longitudinal and hoop steel, respectively, with respect to the gross sectional area.

Table 6 Proposed Principal Tension Stress Values for Outrigger Beam Assessment

Principal Tension Stress	Condition
$p_t = 6.0\sqrt{f_c^{'}}\,psi$ $p_t = 0.50\sqrt{f_c^{'}}\,MPa$	Outrigger beam cracking

RETROFIT RECOMMENDATIONS FOR OUTRIGGER KNEE JOINTS

INTRODUCTION

This section provides retrofit guidelines for improving the seismic performance of outrigger knee joints in existing bridges. The thickness of steel jacket required to develop a well-controlled ductile hinging mechanism in the columns, the requirements to establish a stable joint force transfer mechanism between the column and the beam reinforcement in the closing and the opening directions, and recommendations to avoid potential failure modes in the joint region and the neighboring elements are discussed. Design and detailing guidelines for the retrofit of outrigger knee joints, for both regular and split outrigger bents, are then proposed.

RETROFIT DESIGN CRITERIA

Retrofit to Provide Force Transfer Through the Joint

Analysis of the force transfer from beam to column using equilibrium equations based on the assumption of isotropic material behavior of concrete knee joint is only valid prior to cracking (Priestley et al, 1996). Cracking of the concrete, which occurs when principal tension stresses exceed the joint concrete tension strength, along with the inelastic behavior of both the concrete and the reinforcement embedded in the joint, make the analysis of the force flow through the joint more difficult. Therefore, a rational evaluation of the force flow through knee joints is required.

Closing moments

The approach presented here follows the approach by Priestley (1993) to determine the required horizontal stirrups for knee joints with circular columns subject to closing actions. The approach is modified where needed to address the case for knee joints with rectangular columns retrofitted by a steel jacket.

Under closing of the joint, the column tension force is directly transferred into a diagonal strut, D, within the joint region on the assumption that sufficient confining steel is provided to equilibrate the horizontal force, F_h, as shown in Figure 22.

For rectangular columns with equally distributed reinforcement on all faces or with concentrated reinforcement along the outer faces parallel to the axis of bending, the centroid of the column tension steel can be approximately assumed at an effective depth of $0.85h_{c,}$ as determined from section analysis utilizing the moment-curvature software XTRACT. Based on work by Priestley (1993), the centroid of the tension force transfer

can be assumed to act at a height of $0.7l_a$ to allow for strain penetration, where l_a is the embedment depth of the column reinforcement into the joint region. Then, the required clamping force, F_h, that equilibrates the vertical component of the diagonal strut, D, can be computed by taking the sum of the moments about the centroid of the column compression block, $a_c/2$.

$$F_h = \frac{T_c\left(0.85h_c - \frac{a_c}{2}\right)}{0.7l_a} \qquad \text{(Equation 7)}$$

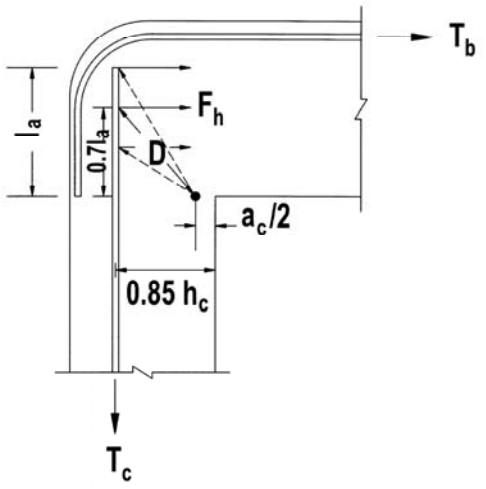

Figure 22 Transfer of Column Tension Force to Diagonal Compression Strut.

According to Priestley (1993), F_h can be assumed to be uniformly distributed over the top 60% of the column embedment length l_a. Thus, the clamping force that can be provided by a circular steel jacket of a thickness t_c, yield strength f_{yh}, and a length of $0.6l_a$ is given by:

$$F_h = 2t_c(0.6l_a)f_{yh} \geq \frac{T_c\left(0.85h_c - \frac{a_c}{2}\right)}{0.7l_a} \qquad \text{(Equation 8)}$$

with simplification: $$t_c \geq \frac{1.19T_c\left(0.85h_c - \frac{a_c}{2}\right)}{l_a^2 f_{yh}} \qquad \text{(Equation 9)}$$

Equation 9 may be further simplified by assuming that $a_c/2$ equals $0.15h_c$. This assumption is based upon section analysis of rectangular columns with the same longitudinal steel arrangement as mentioned previously and using the software XTRACT. Thus:

$$t_c \geq \frac{0.83T_c h_c}{l_a^2 f_{yh}} \qquad \text{(Equation 10)}$$

The tension force in the column bars, T_c, in equation 10 can be determined precisely by a section analysis, such as can be performed using the software XTRACT. Alternatively, T_c can be taken as the tension force corresponding to 50% of the column longitudinal steel area at yield (Priestley, 1993). This is a reasonable approximation since the column bars on the compression side of the neutral axis are well anchored in the diagonal compression strut (Priestley et al, 1996). An overstrength factor of 1.3 is introduced in equation 11 to account for strain hardening of the column reinforcement. Thus,

$$t_c \geq \frac{0.83x1.3x0.5\rho_l A_{col} f_y h_c}{l_a^2 f_{yh}} \qquad \text{(Equation 11)}$$

or $$t_c \geq \frac{0.54\rho_l A_{col} h_c}{l_a^2}\frac{f_y}{f_{yh}} \qquad \text{(Equation 12)}$$

An additional mechanism can be relied on to transfer the column tension force into a diagonal strut in the joint if the top beam steel is extended down to the bottom of the beam. Such detailing will help in transferring the tension force in the outer column

bars by bond to the tails of the beam bars given that the beam steel area is adequate, as shown in Figure 23. For this situation, Priestley (1993) suggested that 50% of the column tension force, T_c, be carried to the beam bars by bond and the other 50% be transferred by a clamping force. Consequently, the thickness of the steel jacket given by equation 12 can be reduced by ½:

$$t_c \geq \frac{0.27 \rho_l A_{col} h_c}{l_a^2} \frac{f_y}{f_{yh}} \qquad \text{(Equation 13)}$$

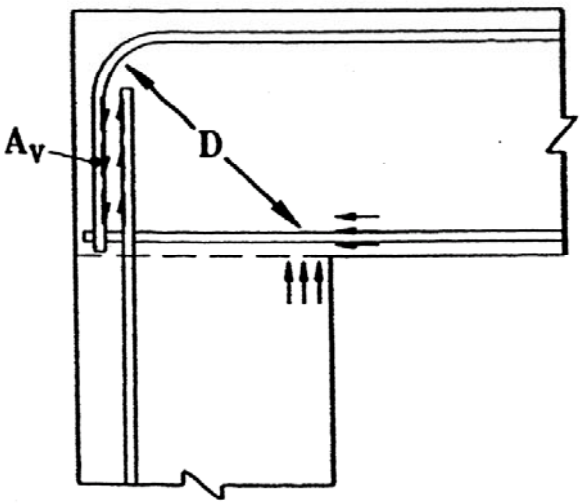

Figure 23 Transfer of Column Tension Force by Bond to Beam Steel (Adapted from Priestley, 1993).

Opening Moments

When a knee joint is subject to opening moments, an arch cracking pattern develops between the compression zones of beam and column. This was evident during tests on the nominally unreinforced knee joints under in-plane loading conducted in this study and that conducted by Ingham (1995). A potential failure mechanism of nominally unreinforced knee joints under opening moments is of concern when the column reinforcement is terminated below the beam compression force, as is the case in most

knee joints in older bridges. Concrete covering the column reinforcement can split off the joint through the initiation of a horizontal crack at the top level of the column rebars, as shown in Figure 24 (Priestley, 1993).

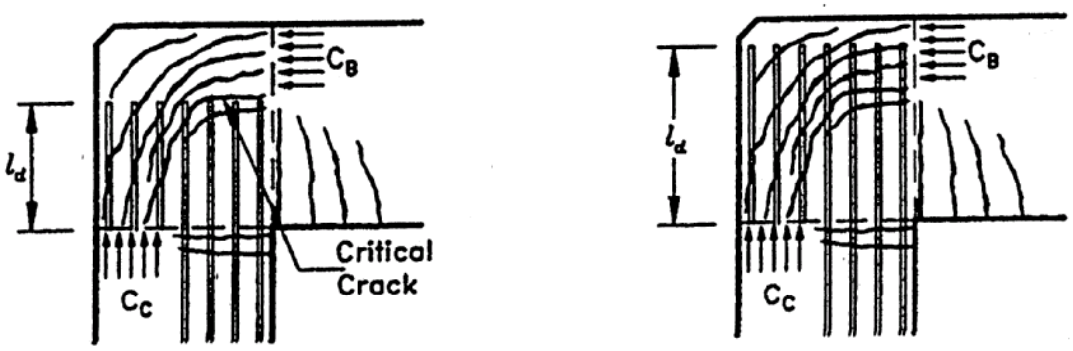

Figure 24 Cracking Pattern Under Opening of the Joint for Insufficient and Sufficient Embedment Rebar Lengths (Adapted from Ingham, 1995).

To avoid this kind of failure, Priestley (1993) proposed three mechanisms to transfer the column tension force into a diagonal strut, *D*, between the beam and the column compression forces. Knee joint reinforcement for each mechanism is shown in the following figure.

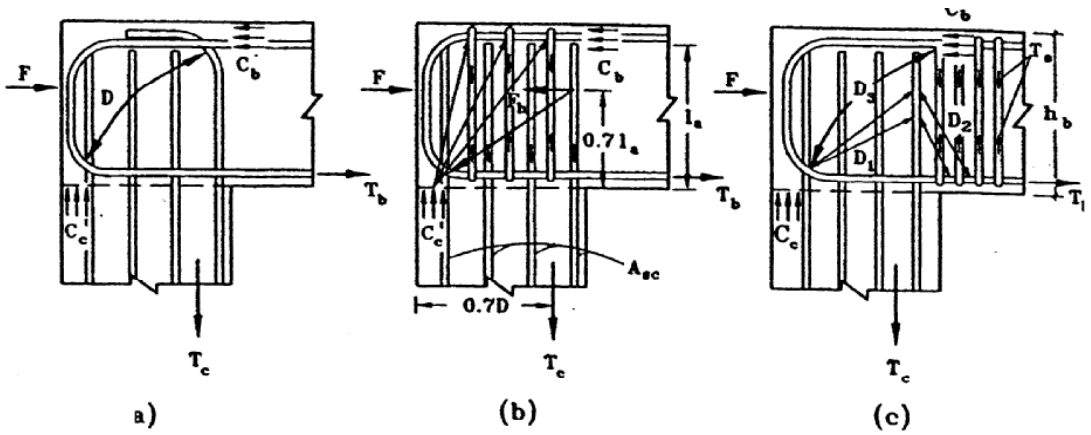

Figure 25 Knee Joint Reinforcement Under Opening Moments (Adapted from Priestley et al, 1996).

In the first mechanism shown in Figure 25a, the column reinforcement adjacent to the beam is bent over the joint to provide the required vertical component to C_b. The second reinforcement scheme incorporates the use of vertical joint reinforcement to transfer part of the column tension force, T_c, by bond up to the top of the joint, as shown in Figure 25b. In the last alternative, vertical reinforcement is provided outside the joint in the outrigger beam to support the formation of a diagonal compression strut outside the joint, as shown in Figure 25c. The third force transfer mechanism was employed in this study to determine the required thickness of the beam-joint steel jacket. This third mechanism was selected because the first reinforcement scheme can be utilized only for new designs, and the second alternative results in large amounts of vertical joint reinforcement (Priestley, 1993). The following discussion summarizes the approach followed by Priestley (1993) to determine the reinforcement needed to satisfy the force transfer mechanism in the third arrangement. This approach is then extended to address the use of circular jackets around the beam and the joint.

As shown in Figure 26, anchorage of the column bars adjacent to the beam is provided by struts D_1 and D_2. The vertical component of strut D_2, equal to T_s, provides the required force to balance the main strut D_3 from C_b towards C_c. T_s is provided by placing stirrups within a distance $h_b/2$ in the beam region from the beam joint interface in addition to that required for shear. Priestley et al (1996) recommended that 50% of the tension force in the column, $0.5T_c$, should be transferred by this mechanism, half of which is transferred through strut D_1 and the other half via strut D_2. The tension force carried by the beam stirrups is then $T_s = 0.25T_c$. T_c can be approximated as $0.5A_{sc}f^o_{yc}$, where A_{sc} is column longitudinal reinforcement area and f°_{yc} is the overstrength stress in

the column bars, which includes strain hardening and yield overstrength (Priestley et al, 1996).

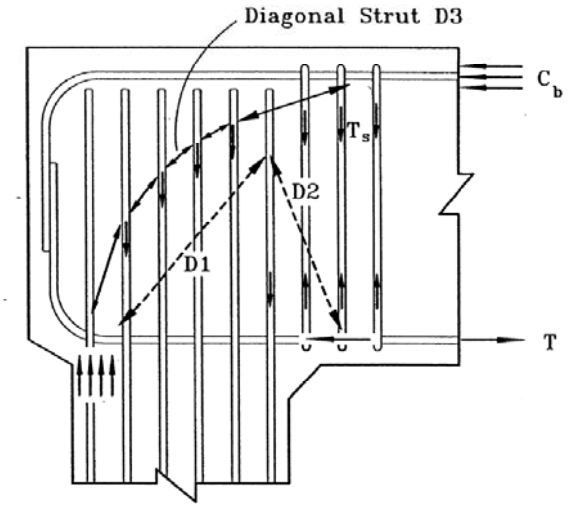

Figure 26 Force Transfer Mechanism In a Knee Joint Under Opening Moment (Adapted from Priestley et al, 1996).

This approach can be extended to deal with circular jackets by equating the tension force in the steel jacket at yield over a length of $h_b/2$ with the required vertical component force, T_s. Thus:

$$T_s = 2t_b \frac{h_b}{2} f_{yh} = 0.125 A_{sc} f_{yc}^o \qquad \text{(Equation 14)}$$

with simplification:

$$t_b \geq \frac{0.125 A_{sc}}{h_b} \frac{f_{yc}^o}{f_{yh}} \qquad \text{(Equation 15)}$$

where t_b is the required jacket thickness around the beam in the joint vicinity.

To ensure bond transfer of the top reinforcement, vertical stirrups are to be provided in the joint area. These stirrups are designed to resist a total force equal to 50% of T_s (Priestley et al, 1996). Again, this recommendation can be extended to address the

situation in which the joint is reinforced with a circular jacket rather than vertical stirrups. In the case of a circular jacket, the vertical force, $0.5T_s$, results in a bending force in the beam jacket, compression on the top face, and tension on the bottom face. Assuming that the vertical force acts at the centroid of the column, the resulting moment at the beam joint interface equals $0.5T_sh_c/2$. The force created in the jacket, F, can be computed by resolving the moment into a tension and a compression component couple over the depth of the steel jacket, that is, the diameter of the jacket. Thus:

$$F = \frac{0.0625 A_{sc} f_{yc}^{o} h_c}{2D} \qquad \text{(Equation 16)}$$

To support this force, the joint jacket is extended below the bottom of the beam jacket. The required joint jacket thickness can be calculated by equating F with the force provided by the lip length of the joint jacket (i.e., the portion below the bottom of the beam jacket) at yielding. For a lip distance of 6 in. (150 mm), the required thickness is equal to:

$$6\,(2 f_{yh} t_{o1}) = \frac{0.0625 A_{sc} f_{yc}^{o} h_c}{2D} \qquad \text{(Equation 17)}$$

with simplification:

$$t_{o1} = \frac{A_{sc} h_c}{380D} \frac{f_{yc}^{o}}{f_{yh}} (in.; psi) \qquad \text{(Equation 18a)}$$

$$t_{o1} = \frac{A_{sc} h_c}{9600D} \frac{f_{yc}^{o}}{f_{yh}} (mm; MPa) \qquad \text{(Equation 18b)}$$

Note that the recommendation on the lip distance was obtained from tests on the retrofitted knee joints of this study.

The requirements of equations 18a and 18b are not onerous, and other equations will, for most cases, control the design of the jacket thickness. Note also that the

compression component of the moment in the steel jacket is not considered here as it is counteracted by the horizontal component of the strut D_1. If vertical stirrups were utilized for the joint design instead of circular jackets, it would be required to provide additional beam bottom reinforcement to sustain the mechanism discussed here. The additional reinforcement for the horizontal component of the strut D_1 is discussed in detail by Priestley (1993).

Priestley et al (1996) recommended providing horizontal reinforcement to the joint that is able to resist 50% of the clamping force required in the closing direction. This is to counteract the outward thrust resulting from the difference in the horizontal components of struts D_1 and D_2. Thus:

$$t_{o2} \geq \frac{0.14 \rho_l A_{col} h_c}{l_a^2} \frac{f_y}{f_{yh}} \qquad \text{(Equation 19)}$$

This requirement is already satisfied by equation 13 when designing the joint jacket for the closing direction mechanism.

In conclusion, for a dependable force transfer mechanism in the opening direction, the steel jacket thickness around the beam and the joint should satisfy the greatest thickness required from equations 15, 18a or 18b, and 19.

Retrofit to Provide Anchorage of Column Longitudinal Steel

Development length may be defined as the distance over which a bar must be bonded to develop the stress in the bar at the overstrength capacity of the member. This length is dependent upon a number of factors, including bar diameter, tensile strength of the concrete and lateral confinement stress around the bar.

Lateral confinement enhances the development of reinforcement by restraining

the dilation of the splitting cracks around the bars. Results of experiments on confined bars in elements under seismic loading showed that much shorter development lengths are needed in confined conditions than for unconfined conditions (Paulay and Priestley, 1992). In knee joints, confinement for column bars adjacent to the beam is provided by the surrounding concrete and transverse reinforcement in the beam itself. For column bars on the other faces, transverse reinforcement should be provided.

According to Priestley et al (1996), the amount of transverse reinforcement required to transfer the column bar stress to the concrete by shear friction can be obtained by equating the clamping force provided to each bar by hoops distributed over an anchorage length of l_a, as shown in Figure 27, to the overstrength bar capacity. For circular columns, the clamping force provided to a bar by a single hoop of area A_h and stress f_s is equal to $A_h f_s 2\pi/n$, while the overstrength bar capacity is $A_b f^o_{yc}$ where A_b is the bar area, fs is equal to 0.0015 times the modulus of elasticity of the steel bars, and n is the number of column longitudinal bars. Assuming a coefficient of shear friction, μ, equal to 1.4, the required area of transverse reinforcement, A_h, can be determined by the following equation (Priestley, 1993):

$$\mu \frac{A_h f_s 2\pi}{n} \frac{l_a}{s} = A_b f^o_{yc} \qquad \text{(Equation 20)}$$

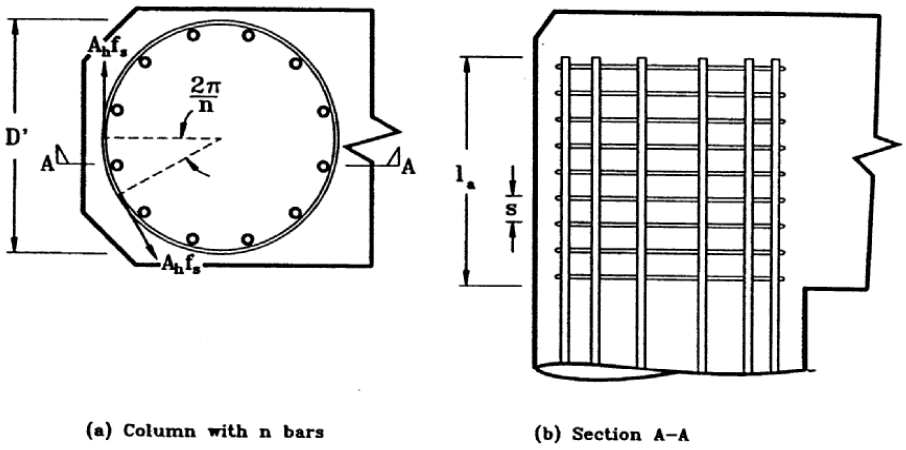

Figure 27 Anchorage by Lateral Confinement (Adapted from Priestley et al, 1996).

Equation 20 can be modified to address rectangular columns confined by a steel jacket using the same methodology developed by Priestley. The clamping force provided to a bar by a steel jacket of thickness t and stress f_s over a length of l_a is equal to $tl_a 2\pi/n$. Note that the clamping force here represents an average value rather than an exact value, as the case in circular columns, because the $2\pi/n$ term in the clamping force expression is not the same for every segment in a rectangular column, as shown in Figure 28. Thus, equation 20 then can be expressed as:

$$\mu t f_s l_a \frac{2\pi}{n} = A_b f_{yc}^o \qquad \text{(Equation 21)}$$

Setting μ to 1.4 as proposed previously, expressing nA_b as A_{sc}, and rounding up coefficients, equation 21 can be rewritten as:

$$t \geq \frac{0.11 A_{sc} f_{yc}^o}{f_s l_a} \qquad \text{(Equation 22)}$$

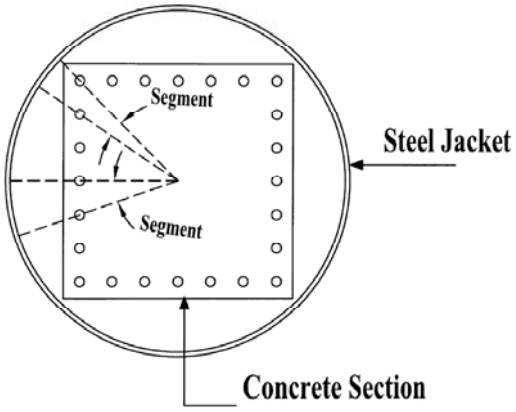

Figure 28 Rectangular Column Confined by a Steel Jacket.

Retrofit for Flexural Ductility Enhancement

Plastic hinge zones provide deformation and energy dissipation capacity to structural systems. The ability of a plastic hinge to sustain large inelastic rotations and curvatures is a function of the level of confinement pressure provided. A number of studies have been conducted on older bridge columns to investigate the effectiveness of retrofit techniques on flexural ductility and flexural integrity of column lap splices. The retrofit techniques include steel jacketing, reinforced concrete jacketing and composite-material jackets involving fiberglass and carbon fiber. Among those, steel jacketing is the most commonly used technique for retrofitting deficient concrete columns.

Research by Priestley and Seible (1991) has shown that the steel jacketing is a very successful method of retrofitting reinforced concrete columns. The technique, which was originally developed for circular columns, used two half-shells of steel plate rolled to a radius that is 0.5 in. (13 mm) to 1.0 in. (25 mm) larger than the column radius and site welded along the vertical seams. Typically, a 2.0-in. (51-mm) gap is provided between the jacket and the neighboring member (e.g., footing or beam) to avoid the

possibility of the jacket acting as a compression reinforcement by bearing against the supporting member at large drift angles. The difference between the jacket and the column is then grouted with a cement grout after flushing with water. Usually, partial height jackets are used to improve the hinge and/or splice region performance. The jacket provides the deficient area in the column with the necessary confinement by acting as passive confinement. That is, a reaction is created in the steel jacket due to lateral expansion of the compressed concrete as a result of high axial compression strains or the tensioned concrete as a function of dilation of lap splices under incipient splice failure.

For rectangular columns, circular or elliptical steel jackets are recommended over rectangular steel jackets (Priestley et al, 1996). Rectangular steel jackets provide confinement to the section through the bending action of the jacket sides, which is significantly more flexible than the circumferential continuous tension action in circular or elliptical sections.

Priestley et al (1996) developed equations for the design of circular and elliptical steel jackets. For confinement of plastic hinge regions, the equation basically relates the volumetric confinement ratio to the required plastic curvature of the critical section in the column. A conservative material-dependent relationship between ultimate compression strain and volumetric ratio of jacket confinement was then employed to solve for the jacket thickness, t_j:

$$t_j = \frac{0.18(\varepsilon_{cm} - 0.004)Df'_{cc}}{f_{yj}\varepsilon_{sm}} \qquad \text{(Equation 23)}$$

where ε_{cm} = the maximum compressive strain required in the hinge, D = the jacket diameter, f'_{cc} = the confined concrete compressive strength, f_{yj} = jacket yield strength

and ε_{sm} = jacket strain at maximum stress. Design charts for required steel jacket thickness for circular columns are given in Figure 29 as functions of column longitudinal reinforcement ratio and axial load ratio. The figure was constructed for Grade 40 (276 MPa) and two common longitudinal bar sizes and for A36 steel jacketing based upon extreme deformation requirements (an approximate total drift of 5%).

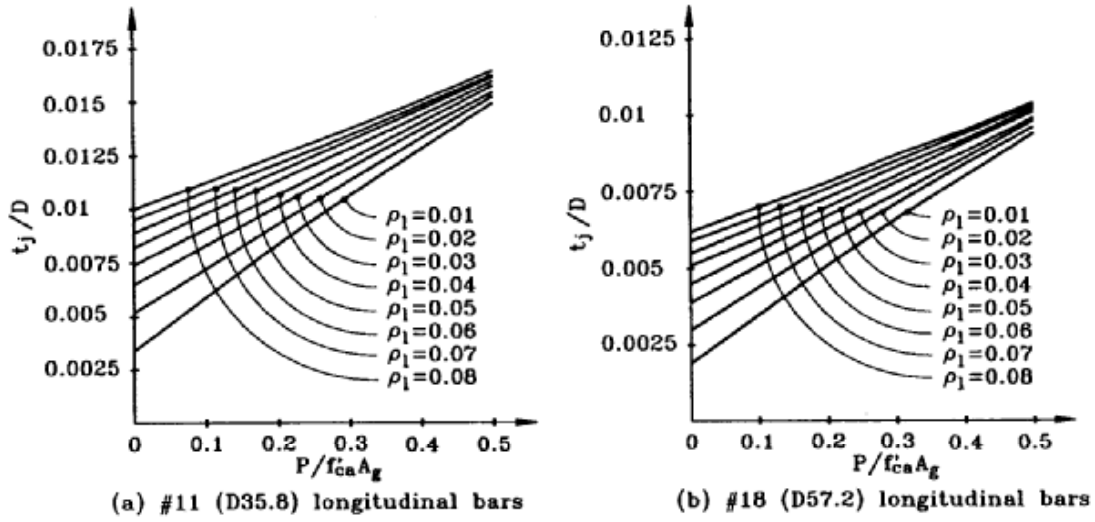

Figure 29 Steel Jacket Thickness to Provide a Plastic Drift of 4.5% in a Circular Column (Adapted from Priestley et al, 1996).

Retrofit for Anchorage of Beam Reinforcement

Under closing of the joint, the tension force in the beam reinforcement extending into the joint region results in radial stresses on the concrete below the bend, as shown in Figure 30 (Priestley, 1993). In such a case, the beam hook extensions will bend out unless adequate restraint to these bars is provided. Priestley (1993) suggested providing the joint with horizontal reinforcement that is capable of restraining the beam hook extension at the plastic moment capacity of the beam bars. The joint horizontal reinforcement is distributed over a length of $12d_b$, where d_b is the diameter of the beam

bar. Assuming no contribution from the concrete cover, the force, F_R, required to restrain one bar is equal to (Priestley, 1993):

$$F_R \geq \frac{1.3\pi d_b^2 f_y}{120} \qquad \text{(Equation 24)}$$

Extending this approach to joints retrofitted using circular jackets, the required restraining force for n number of beam hooks can be supplied by a steel jacket of thickness, t_j, and a length of $12d_b$. Thus:

$$2 f_{yh} t_j (12 d_b) \geq \frac{1.3\pi d_b^2 f_y}{120} n \qquad \text{(Equation 25)}$$

simplifying and approximating numbers yields:

$$t_j \geq \frac{n d_b}{700} \frac{f_y}{f_{yh}} \qquad \text{(Equation 26)}$$

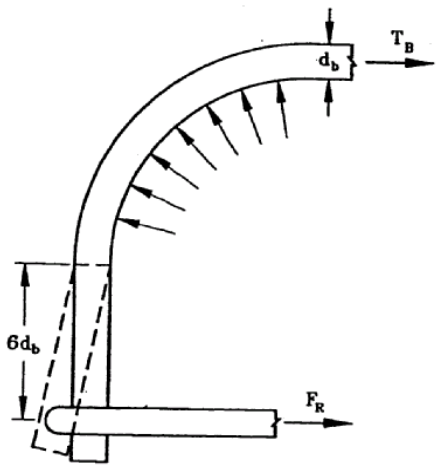

Figure 30 Beam Hook Extension Restraint (Adapted from Priestley, 1993).

Retrofit of Outrigger Beam

Under out-of-plane loading, an outrigger beam is subjected to bending, torsion and shear forces. When the magnitudes of two or more of the forces are relatively large, the effects under combined loading must be considered in the design. Design procedures for members under combined loading generally are in the form of nondimensionalized interaction equations based on the strength of the section. For designing reinforced concrete members under combined loading, Hsu (1983) proposed the following interaction equation:

$$\frac{M}{M_o}+\left(\frac{T}{T_o}\right)^2 R+\left(\frac{V}{V_o}\right)^2 R \le 1 \qquad \text{(Equation 27)}$$

where M, T and V are the moment, torsion and shear design forces, respectively; M_o, T_o and V_o are the pure bending, torsion and shear strengths of the member, respectively; and R is the ratio of the tensile and compressive forces in the beam at yield.

Equation 27 can be used to determine the required beam steel jacket thickness to carry the beam loads. Demand forces on the most critical outrigger beam section should be computed based upon the overstrength capacity of the column hinge section. Bending, torsion and shear strengths of the reinforced concrete beam with circular steel jacket can be calculated assuming composite action of the existing beam section and the steel jacket.

Based on work by Priestley et al (1996), the shear strength contribution of a circular steel jacket, V_{sj}, used for retrofitting purposes can be computed by the following equation:

$$V_{sj}=\frac{\pi}{2}t_j f_{yj} D\cot\theta \qquad \text{(Equation 28)}$$

where t_j is the thickness of the jacket, f_{yj} is the yield strength of the jacket, D is the

diameter of the jacket, and θ is the angle of the critical inclined flexure shear cracking to the column axis taken as 35˚.

In torsion, the torsion moment contribution of a circular steel jacket can be computed using the thin tube analogy. From Hsu (1983), the torsion yield contribution of the jacket, T_{jy}, is:

$$T_{jy} = 2A_j t_j f_{yj} \qquad \text{(Equation 29)}$$

where A_j is the area enclosed within the centerline of the jacket. Shear and torsion strengths of the existing reinforced beam section are not discussed here as they are presented explicitly in the ACI 318-02 code provisions (2002).

Finally, in bending, the strength capacity of the beam section after retrofitting can be determined using moment capacity analysis, easily obtained using software such as XTRACT.

SUMMARY OF OUTRIGGER KNEE JOINT SYSTEM RETROFIT DESIGN

The purpose of the seismic upgrade of the outrigger bents is to minimize damage in the knee joint and in the outrigger beam, presuming that the column in the outrigger bent has already been retrofitted, and to enhance the ductility and the energy dissipation capacity of the system under in-plane and out-of-plane loading. The retrofit measures proposed in this study incorporate the use of an elbow-shaped steel jacket around the beam and the joint region. The following discussion provides a summary of the recommended guidelines for the design and detailing of the steel jacket around the beam and the joint.

Regular outrigger bents

Scope: The retrofit measures presented here are applicable to outrigger bents with columns and beams of similar size sections. For other cases, the approach will lead to two jackets, the column jacket and a jacket over the beam and the joint, that are different in size.

Design forces: Component demand forces should be determined based on the development of the overstrength capacity of the column hinge section in each direction. The overstrength capacity can be obtained from a section analysis of the column hinge section using characteristic material strengths and including the effect of confinement on the strength of the concrete. The characteristic yield strength can be taken as $1.1f_y$ and $1.3\,f_c^{'}$ for the steel and the concrete, respectively (Priestley et al, 1996). A strength reduction factor of $\phi = 1.0$ may be used in the design process since demand actions are determined based on conservative material properties (Ingham and Sritharan, 2003).

Column retrofit: The plastic hinge location at the top of the column should be located at a distance of 1/3 of the larger column side dimension below the beam-joint interface or 6 in. (150 mm) below the beam jacket, whichever is larger, as shown in Figure 31. This limit on the plastic hinge location is introduced so as to locate the hinge as close as possible to the maximum moment location while at the same time provide enough lip distance for the joint. The purpose of the lip is to provide a reaction area for the compression strut between the column and the beam reinforcement. For outrigger bents with jacketed columns, the gap is provided by removing the existing column jacket and grout to the depth of original column. For new retrofits, the column jacket is terminated

at the appropriate location. A gap width of 2 to 4 in. (50 to 100 mm) is recommended in order to prevent contact between the jackets at large drift ratios and to avoid excessive flexural strength enhancement of the plastic hinge region.

Beam-joint retrofit: The beam-joint jacket is constructed from two clamshell-sections fabricated offsite and field welded together with a full capacity weld. The clamshells are fabricated by formulating a pipe section through curving a flat plate to the required radius and length that covers both the beam and the joint. The pipe is then cut at a 45-degree angle to the required length to jacket the beam. The remaining part of the pipe (eventually forming the joint jacket) is rotated 90-degrees in plane and 180-degrees out-of-plane to form an elbow shape together with the beam jacket. The two pieces are then welded together using a full capacity weld. The resulting final shape of the jacket is shown in Figure 32.

The shape and size of the jacket are determined based on the shape and size of the beam section. For optimal strength, confinement and use of the materials, circular steel jackets are recommended for beams with square sections or rectangular sections with approximately the same side lengths, while elliptical jackets are recommended to encase beams with oblong rectangular sections. For circular or elliptical jackets, the size of the jackets can be reduced by chipping off the corners of the beam.

The beam jacket may overlap any existing column jacket above the hinge location, as shown in Figure 31. A gap of 2 to 4 in. (50 to 100 mm) should be maintained between the beam jacket and the superstructure to prevent contact at large drift angles.

The space between the jacket and the joint and the beam is filled with a high-strength, non-shrinkage grout. The grouting sequence is a function of the construction

procedures and the type of the grout used. The sequence of grouting should be selected so as to insure complete filling of the void spaces.

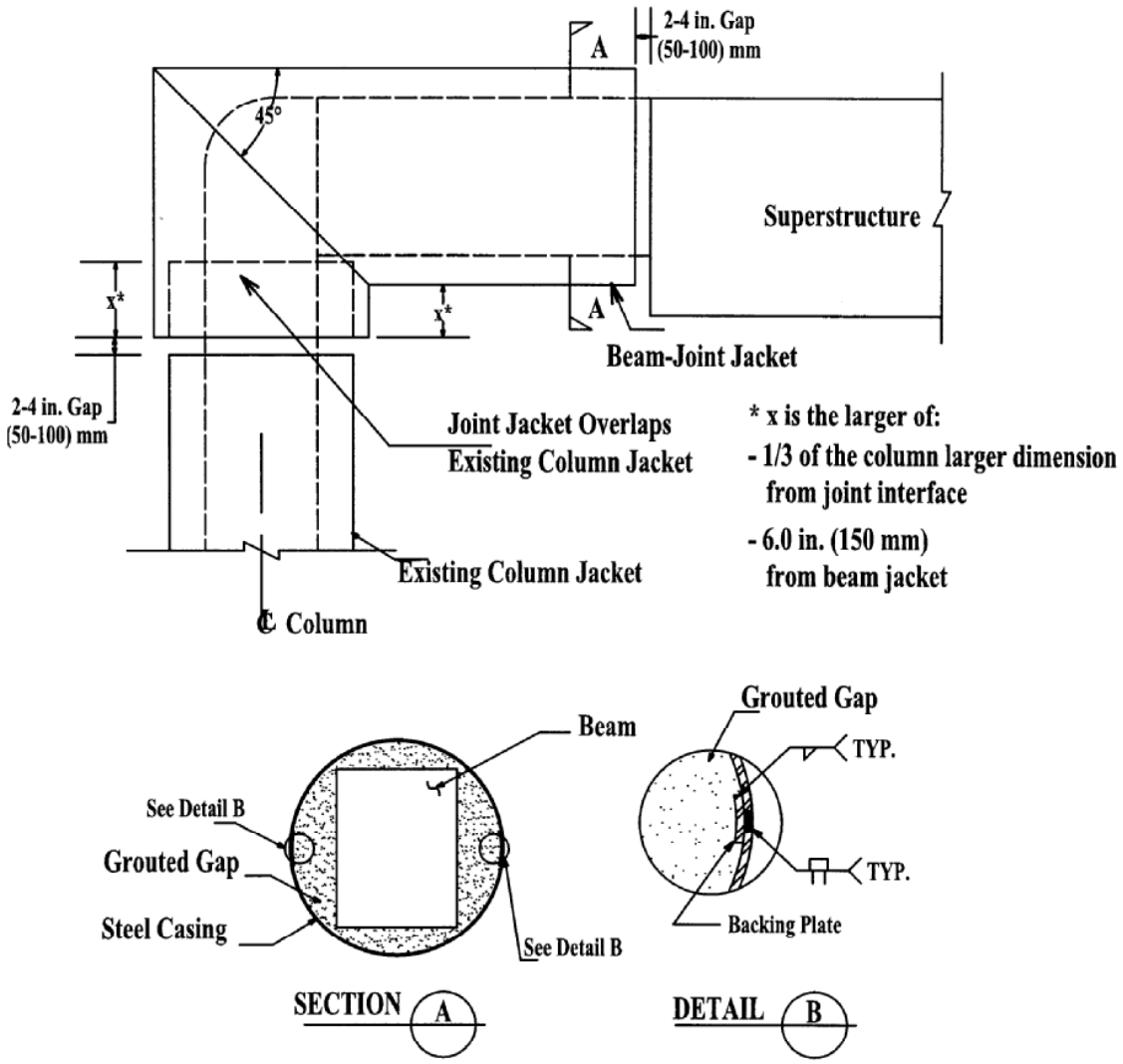

Figure 31 Steel Jacket Retrofit Details.

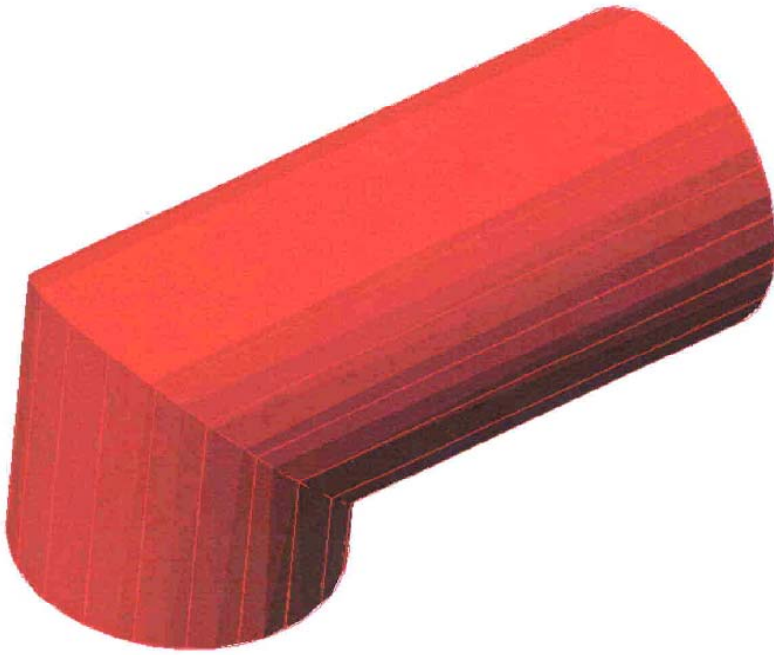

Figure 32 Isometric shape of the Beam-Joint Steel Jacket.

Jacket thickness: The thickness of the jacket is chosen as the largest of:

1. The thickness of the existing column jacket.
2. The thickness that enables a stable force transfer mechanism between the column and the beam in the closing and the opening directions using equation 13 is for closing of the joint and equations 15, 18a or 18b, and 19 are for the opening direction. The requirements of item 1 or item 2 will, most likely, control the required jacket thickness.
3. The thickness necessary for providing sufficient confinement for anchorage of the column rebars into the joint, equation 22.
4. The thickness that generates an effective confinement pressure around the column joint interface equal to that provided by the column jacket over the hinge location, equation 23.

5. The thickness required for anchorage of beam reinforcement, equation 26.
6. The thickness needed to assure that the nominal capacity of the upgraded beam is greater than the ultimate demand on the beam taking into consideration the interaction of bending, shear and torsion forces, equation 27.

Connection to superstructure: The connection of the retrofitted outrigger knee joint system to the bridge superstructure should be evaluated. Some retrofitting may be needed to ensure transfer of the forces from the upgraded outrigger bents to the bridge superstructure. The ultimate forces transferred to the bridge superstructure from the upgraded outrigger knee joint systems can be quantified based on the ultimate capacity of the column hinge. An overstrength factor of at least 25% is recommended in estimating the ultimate capacity of the plastic hinge for capacity design of the connection.

Split outrigger bents

The guidelines developed for regular outrigger bents can also be utilized to upgrade split outrigger bents:

Scope: Same as for regular outrigger bents.

Design forces: Same as for regular outrigger bents.

Column retrofit: Similar to regular outrigger bents, the plastic hinge location at the top of the column should be located at the larger of: 1/3 of the larger column side dimension below beam-joint interface or 6 in. (150 mm) below the beam jacket, as shown in Figure 33. For split outrigger bents with existing column jackets, the gap is provided by removing the circular part of the existing D-shaped column jacket and grout to the depth of the original column. Additionally, the flat plate on the inner surface of the column in

the gap hinge region should be cut off to the depth of the original column. For new retrofits, the column jacket is terminated at the appropriate location. The width of the gap is recommended to be between 2 to 4 in. (50 to 100 mm).

Beam-joint retrofit: The beam-joint jacket is a D-shaped steel jacket consisting of a clamshell- section and a flat plate of the same thickness. The flat plate is adhered to the back face of the beam and the joint, using high-strength epoxy, and then field welded to the clamshell with a full capacity weld. A picture of a clamshell section is shown in Figure 34.

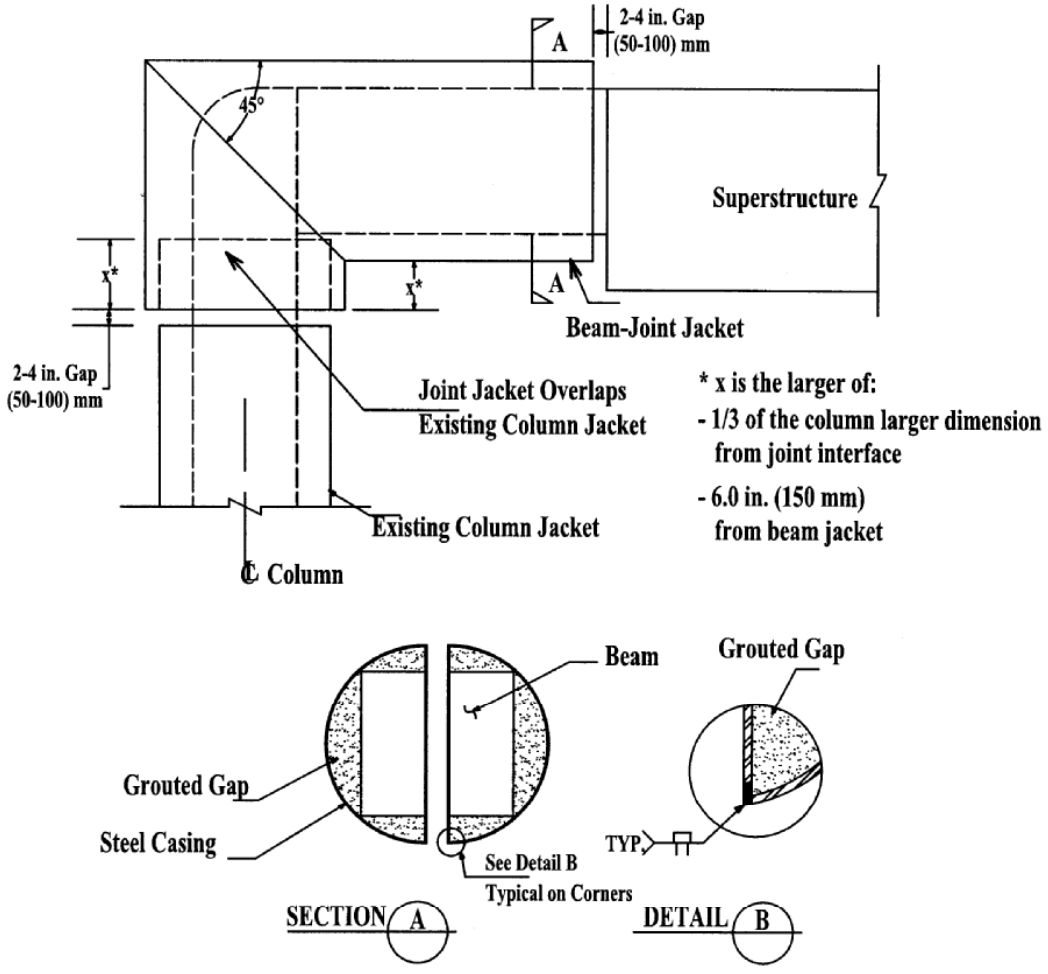

Figure 33 Steel Jacket Retrofit Details.

Figure 34 A Picture of the Clamshell Used in the Retrofit of the Beam-Joint.

The flat plate on the inner face of the beam should be bent out at a 45-degree angle ahead of the beam joint interface to account for any increase in the size of the joint over the beam. Due to the existing steel jacket being behind the column, the plate behind the joint is cut off at the column joint interface level. Another rectangular plate projecting out a distance equal to the thickness of the existing plate behind the column is fillet welded at the shop to the big plate. A picture of a flat plate with these details is shown in Figure 35.

The size of the jacket is determined based on the size of the beam section. The diameter of the circular part in the D-shaped casing can be reduced by chipping off the corners of the beam.

Similar to regular outrigger bents, the beam jacket may overlap existing column jackets above the hinge location, as shown in Figure 33. A gap of 2 to 4 in. (50 to 100 mm) should be maintained between the beam jacket and the superstructure.

The space between the jackets and the joint and the beam is filled out by a high-strength, non-shrinkage grout. The grouting sequence should provide for complete filling of the void spaces.

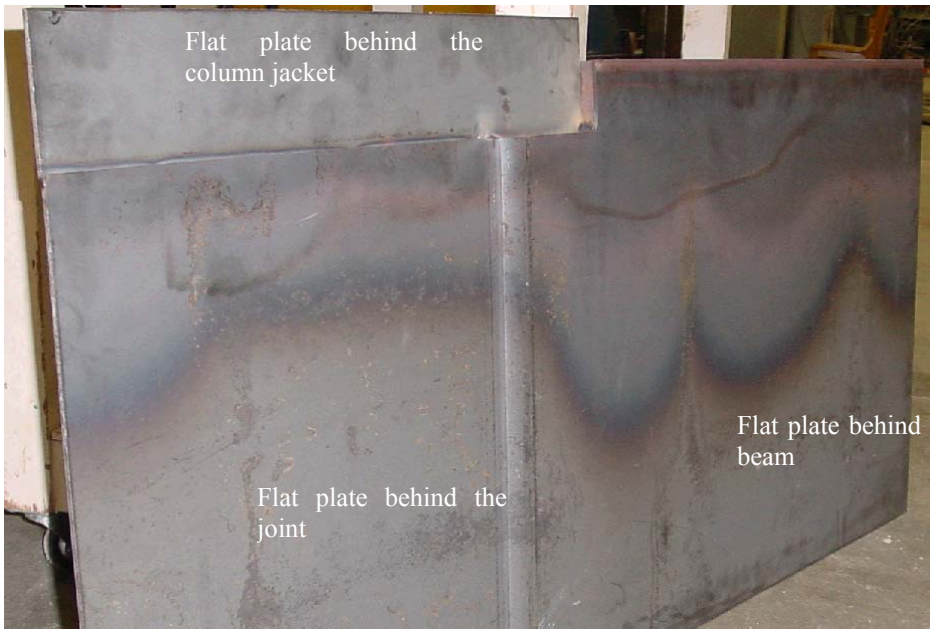

Figure 35 A Picture of the Flat Plate Used in the Retrofit of the Beam-Joint.

Jacket thickness: Same as for regular outrigger bents.

Split gap: It is required to maintain at least a gap of ½ in. (15 mm) between the split outrigger after retrofit to account for any longitudinal movement in the adjacent bridge specimens.

Connection to superstructure: Same as for regular outrigger bents.

CONCLUSIONS

The experimental test results of this study indicate that outrigger bents with reinforcement details typical of those present in the Spokane Street Overcrossing will likely perform poorly in a significant earthquake event. Tests carried out on specimens with short and long outrigger beams representing as-built conditions showed that shear cracks will form in the joint region at low displacement levels. Failure will happen as a result of bond splitting of the column reinforcement hook extensions within the joint due to inadequate confinement, thereby resulting in a system with low ductility and energy dissipation capacities. The existing outrigger knee joint systems can be expected to have a maximum ductility level in the range of 2.0 to 2.8. In the case of out-of-plane motion in the longitudinal direction of the bridge, the outrigger beams will experience cracking at low displacement levels. Bond splitting failure of beam reinforcement in the joint due to inadequate confinement along with the low torsional strength of the beam will result in the potential for failure of the system. Test results indicate that the existing knee joint systems with short outriggers will attain a capacity that is approximately 50% higher than the torsion cracking strength of the beam.

Circular and D-shaped steel jacketing around the beam and the joint of regular and split outrigger bents, respectively, prevented bond splitting failure of the column bars within the joint and increased the torsional strength of the outrigger beam. The steel jackets were effective in improving the displacement ductility, drift, strength and energy dissipation capacities of the system under in-plane and out-of-plane loading when compared to the response of the as-built specimens. The retrofitted outrigger knee joint

systems can be expected to achieve ductility levels of at least 5 as well as drift capacities exceeding 6%.

Results from this research showed that the proposed threshold principal tension stress values for seismic assessment of unreinforced knee joints are somewhat higher than those developed by Priestley (1993) due to the beam side reinforcement extending into the joint. Therefore, for knee joints where the beam side reinforcement is fully developed into the joint region and having a longitudinal steel ratio around 0.45%, seismic assessment may be conducted based upon the threshold values proposed in this study. For cases where the beam side reinforcement terminates at the joint interface, values developed by Priestley (1993) should be utilized.

RECOMMENDATIONS/APPLICATIONS/IMPLEMENTATION

Joint principal tension stress was linked to the joint condition of the as-built specimens under in-plane loading. Joint principal tension stress is determined based on a simple Mohr's circle analysis as discussed by Priestley et al (1996). Principal tension stress values of $4.5\sqrt{f_c'}$ psi ($0.38\sqrt{f_c'}$ MPa) and $6.0\sqrt{f_c'}$ psi ($0.50\sqrt{f_c'}$ MPa) were set as limits beyond which joint shear cracking and joint failure, respectively, are expected.

For outrigger beams with reinforcement details typical to those present in the Spokane Street Overcrossing, a principal tension stress value of $6.0\sqrt{f_c'}$ psi ($0.50\sqrt{f_c'}$ MPa) is proposed as a limit after which torsion cracking in the beam can be expected. The principal tension stress is determined based on contributions from shear and torsion stresses. The ultimate capacity of the outrigger beams, T_n, can be taken as:

$$T_n = 1.5T_{cr} \qquad \text{(Equation 30)}$$

where T_{cr}, is the cracking torsional strength of the beam determined based on work by Hsu (1990).

The thickness of the jacket should satisfy the requirements to establish a stable joint force transfer mechanism between the column and the beam reinforcement and to prevent potential failure modes in the joint region and connecting elements. The beam-joint jacket should be the greatest of the thickness requirements discussed in the following paragraphs.

A required steel jacket thickness to establish a reliable force transfer mechanism between the column and the beam reinforcement in the closing and the opening directions was developed in this study. For closing events, the required joint jacket thickness, t_c, is given by:

$$t_c \geq \frac{0.27\rho_l A_{col} h_c}{l_a^2} \frac{f_y}{f_{yh}} \qquad \text{(Equation 31)}$$

where ρ_l is the column longitudinal reinforcement ratio, A_{col} is the column gross sectional area, h_c is the depth of the column parallel to loading direction, l_a is the column embedment length, f_y is the yield strength of the column reinforcement, and f_{yh} is the yield strength of the jacket.

For opening events, the required jacket thickness, t_{o1}, is:

$$t_{o1} = \frac{A_{sc} h_c}{380D} \frac{f_{yc}^o}{f_{yh}} \qquad \text{(Equation 32)}$$

where A_{sc} is column longitudinal reinforcement area, f°_{yc} is the overstrength stress in the column bars as defined by Priestley et al (1996), and D is the diameter of the beam-joint jacket. It is also required for opening events that the jacket thickness, t_b, around the beam in the joint vicinity be:

$$t_b \geq \frac{0.125 A_{sc}}{h_b} \frac{f_{yc}^o}{f_{yh}} \qquad \text{(Equation 33)}$$

The required joint jacket thickness, t, to avoid anchorage failure of the column longitudinal bars is given by:

$$t \geq \frac{0.11 A_{sc} f_{yc}^o}{f_s l_a} \qquad \text{(Equation 34)}$$

The required joint jacket thickness, t_j, to restrain the beam hook extensions is given by:

$$t_j \geq \frac{n d_b}{700} \frac{f_y}{f_{yh}} \qquad \text{(Equation 35)}$$

where n is the number of beam hooks to be restrained and d_b is the diameter of the beam bar.

For flexural ductility enhancement, the required steel jacket thickness can be computed by equations developed by Priestley et al (1996) for application to retrofitting columns.

The demand forces on the beam-joint steel jacket should be determined based on the development of the overstrength capacity of the column hinge section in each direction. For the beam section, this should take into consideration the interaction of bending, shear and torsion forces.

For regular and split outrigger bents, the plastic hinge location at the top of the column should be located at a distance of 1/3 of the larger column side dimension below the beam-joint interface or 6 in. (150 mm) below the beam jacket, whichever is larger. For outrigger bents with jacketed columns, the gap is provided by removing the existing column jacket and grout to the depth of original column. For new retrofits, the column

jacket is terminated at the appropriate location. The width of the gap is recommended to be between 2 to 4 in. (50 to 100 mm).

For both regular and split outrigger bents, the beam jacket may overlap any existing column jacket above the hinge location. A gap of 2 to 4 in. (50 to 100 mm) should be maintained between the beam jacket and the superstructure. The space between the jackets and the joint and the beam is filled out by a high-strength, non-shrinkage grout. For split outrigger bents, it is recommended that a gap of at least ½ in. (15 mm) be maintained between the split outrigger after retrofit to provide for longitudinal movement between the adjacent bridge units.

The connection of the retrofitted outrigger knee joint system to the bridge superstructure was not addressed in this study. However, the connection should be evaluated to ensure transfer of the forces from the upgraded outrigger bents to the bridge superstructure. An overstrength factor of at least 25% is recommended in estimating the ultimate capacity of the column plastic hinge for capacity design of the connection.

ACKNOWLEDGEMENTS

This research was conducted through the Washington State Transportation Center (TRAC) and under contract to the Washington State Department of Transportation (WSDOT). The financial support provided by WSDOT and the technical assistance provided by the project technical monitors, Hongzhi Zhang and Chyuan-Shen Lee, is appreciated.

REFERENCES

AASHTO (2004). *AASHTO Standard Specifications for Highway Bridges*, American Association of State Highway and Transportation Officials, Washington, D.C.

ACI 318-02 (2002). *Building Code Requirements for Structural Concrete (ACI 318-02) and Commentary (ACI 318R-02)*. American Concrete Institute, Detroit, MI.

Caltrans (2004). "Caltrans Seismic Design Criteria (SDC) Version 1.3," California Department of Transportation, Sacramento, California.

FEMA (1997). *NEHRP Guidelines for the Seismic Rehabilitation of Buildings, FEMA 273*; Federal Emergency Management Agency, Washington, D.C.

Hsu, T. T. (1983). "Torsion of Reinforced Concrete," *Van Nostrand Reinhold Company Inc.* New York.

Hsu, T. T. (1990). "Shear Flow Zone in Torsion of Reinforced Concrete," *ASCE Journal of Structural Engineering,* 116(11), 3206-3226.

Ingham, J. (1995). "Seismic Performance of Bridge Knee Joints," Ph.D. Dissertation, The Department of Structural Engineering, University of California, San Diego.

Ingham, J. M., Priestley, M. J .N., and Seible, F. (1994a). "Seismic Performance of Bridge Knee Joints – Volume I," *Rep. No. SSRP 94/12*, University of California, Berkeley, San Diego.

Ingham, J. M., Priestley, M. J .N., and Seible, F. (1994b). "Seismic Performance of Bridge Knee Joints – Volume II," *Rep. No. SSRP 94/17*, University of California, Berkeley, San Diego.

Ingham, M. J., and Sritharan, S. (2003). "Application of Strut-and-Tie Concepts to Concrete Bridge Joints in Seismic Regions," *PCI Journal* 48(4), 66-90.

Nilson, H. A., Darwin, D., and Dolan, C.W. (2003). "Design of Concrete Structures," *McGraw-Hill College.*

Paulay, T., and Priestley, M. J. N. (1992). "Seismic Design of Reinforced Concrete and Masonry Buildings," *John Wiley and Sons, Inc.*

Priestley, N. M. J. (1993). "Assessment and Design of Joints For Single-Level Bridges with Circular Columns," *Rep. No. SSRP 93/02*, University of California, Berkeley, San Diego.

Priestley, M. J. N., and Seible, editors. (1991). "Seismic Assessment and Retrofit of Bridges," *Rep. No. SSRP 91/03*, Department of Applied Mechanics and Engineering Seinces, University of California, San Diego, La Jolla, California

Priestley, M. J. N., Seible, F., and Calvi, G. M. (1996), " Seismic Design and Retrofit of Bridges," *John Wiley & Sons*, Inc. New York.

Priestley, M. J. N., Seible, F., Xiao, Y., and Verma, R. (1994). "Steel Jacket Retrofitting of Reinforced Concrete Bridge Columns for Enhanced Shear Strength – Part 2: Test Results and Comparison with Theory," *ACI Structural Journal* 91(4), 394-405.

Shattarat, Nasim K. (2004). "Seismic Behavior and Retrofit of Bridge Knee Joints," Ph.D. Dissertation, Department of Civil and Environmental Engineering, Washington State University.

Stojadinovic, B. and Thewalt, C. R. (1995)."Upgrading Bridge Outrigger Knee Joint Systems." *Rep. No. UCB/EERC-95/03*, Earthquake Engineering Research Center, University of California, Berkeley, California.

Zhang, H., Knaebel, P. J., Coffman, H.L., VanLund, J.A., Kimmerling, R.E., and Cuthbertson, J.G. (1996). "Seismic Vulnerability Study of the SR 99 Spokane Street Overcrossing," Washington State Department of Transportation, Olympia.